

THE POTENTIAL INFLUENCE OF THE ANTECEDENT TOPOGRAPHY ON THE
NORTHERN BAY SHORELINE OF GALVESTON ISLAND

A Thesis

by

LINDSAY KERSTEN CRITIDES

Submitted to the Office of Graduate and Professional Studies of
Texas A&M University
in partial fulfillment of the requirements for the degree of

MASTER OF SCIENCE

Chair of Committee,	Timothy Dellapenna
Committee Members,	Jens Figlus
	Pete van Hengstum
	Niall Slowey
Head of Department,	Shari Yvon-Lewis

May 2019

Major Subject: Oceanography

Copyright 2019 Lindsay Critides

ABSTRACT

The objective of this study was to determine if the antecedent Pleistocene topography influenced the geomorphic features and evolution of Galveston Island and West Galveston Bay (WGB). Antecedent Pleistocene topographic features were identified by mapping the Pleistocene/Holocene unconformity within WGB using high resolution marine geophysics and sediment cores. This study found three incised-valleys that extend beneath Galveston Island, from east to west: 1) Highland Bayou Incised-Valley, 2) Carancahua Incised Valley and Eastern Halls Bayou Incised-Valley, and 3) Western Halls Bayou Incised-Valley and Chocolate Bayou Incised-Valley. The accommodation space created by the valleys acted as an obstacle the island had to overcome, filling with sediment as it grew westward. The incised-valleys reside beneath the island exhibiting unique geomorphic features (frequency of storm surge channels, embayment size, presence of beach ridges and overwash) generally not found on the island not underlain by incised-valleys. The Pleistocene surface contains Deweyville Terraces (−9 m and −9.5 m), providing evidence the incised-valleys formed in conjecture with the Trinity River Incised-Valley.

The measured shear strength of Beaumont Formation sediment was 5-17.5 times higher than the Holocene fill. The Beaumont Formation is indurated and extremely resistant to erosion, whereas the Holocene fill is relatively uncompacted and highly susceptible to erosion. As a result, the Holocene filled valleys undergo differential compaction, causing enhanced subsidence, making them geotechnically weak zones and susceptible to the formation of storm surge channels and embayments.

The initial formation of storm surge channels along the bay shoreline of Galveston Island began concomitant with the initial formation of Galveston Island, when it was in a narrower,

regressive phase where overwash and breaching were common. The island width reached a critical threshold where breaching was no longer possible, increasing to a width of 1,200 m around 3,300 yBP. This is discerned by beach ridges of this age that have never been breached by overwash channels. The PBR flowed through the western half of WGB from 4,000-6,000 yBP, but Carancahua Reef provided a barrier preventing it from flowing into the eastern half of WGB. After the PBR changed course, its sediment ceased to be deposited in WGB.

DEDICATION

This manuscript is dedicated to my husband, Phillip, who has been my #1 fan since the day we met.

ACKNOWLEDGEMENTS

I would like to thank:

My committee chair, Dr. Tim Dellapenna, who has been a respected mentor to me since I was an undergraduate student. His knowledge and encouragement have helped me during this journey and made me a better scientist.

Committee members, Dr. Jens Figlus and Dr. Pete van Hengstum, and Niall Slowey for their guidance and advice.

I would like to thank my family, friends, and my husband Phillip for providing me with never-ending support and encouragement throughout my years in school. This accomplishment would not have been possible without them.

NOMENCLATURE

WGB	West Galveston Bay
PU	Pleistocene Unconformity
PBR	Paleo-Brazos River
EWGB	Eastern West Galveston Bay
CWGB	Central West Galveston Bay
WWGB	Western West Galveston Bay
HBIV	Highland Bayou Incised-Valley
EBIV	Eastern Halls Bayou Incised-Valley
CIV	Carancahua Incised-Valley
WHBIV	Western Halls Bayou Incised-Valley
CBIV	Chocolate Bayou Incised-Valley
MSL	Mean Sea Level
SLR	Sea Level Rise
SBP	Sub-bottom Profile
yBP	Years Before Present (1950)

TABLE OF CONTENTS

	Page
ABSTRACT	ii
DEDICATION	iv
ACKNOWLEDGEMENTS	v
NOMENCLATURE	vi
TABLE OF CONTENTS	vii
LIST OF FIGURES	ix
1. INTRODUCTION	1
2. BACKGROUND	7
2.1 Barrier Islands and Back-Barrier Systems	7
2.2 History of Transgression in Texas	9
2.3 Incised-Valleys	13
2.4 Pleistocene Unconformity in West Galveston Bay	15
2.5 Holocene Stratigraphic Sequence	17
2.6 Analyses of Bay Shoreline Retreat	18
3. STUDY AREA	20
3.1 Galveston Island	20
3.2 West Galveston Bay	21
4. METHODS	23
4.1 Geophysical Survey	23
4.2 Sedimentary Analysis	25
5. RESULTS	27
5.1 Seismic Results	27
5.2 Interpolated Pleistocene Unconformity – 3D Surface	29
5.3 Geometry of Incised-Valleys	32
5.4 Interpreted Paleo-Brazos River Surface	35
5.5 Geomorphology	38

5.6	Storm Surge Channels.....	40
5.7	Geotechnical Properties	42
5.8	Subsurface Facies.....	43
6.	DISCUSSION.....	49
6.1	Formation and Type of Incised-Valleys	49
6.1.1	Eastern West Galveston Bay.....	49
6.1.2	Central West Galveston Bay.....	50
6.1.3	Western West Galveston Bay	51
6.2	Paleo-Brazos River	53
6.3	Geomorphology	55
6.3.1	Transgressive vs. Regressive Features.....	55
6.3.2	Enhanced Subsidence Over Incised-Valleys and Bay Shoreline Retreat ...	58
6.3.3	Storm Surge Channels.....	59
7.	CONCLUSIONS	65
	REFERENCES	69
	APPENDIX.....	76

LIST OF FIGURES

	Page
Figure 1 Regional Map.....	4
Figure 2 The Barrier Island System	8
Figure 3 Formation and Preservation of Storm Surge Channels.....	10
Figure 4 Types of Incision.....	15
Figure 5 Evidence of Pleistocene Unconformity	16
Figure 6 Breach Sites and Shoreline Erosion Rates Along the Bay Shoreline.....	19
Figure 7 Phases of Island Formation.....	20
Figure 8 Core Location and Survey Map	24
Figure 9 Core/SBP of Jamaica Beach	28
Figure 10 Fence Diagram of Pleistocene Unconformity	30
Figure 11 Pleistocene Unconformity Distribution of West Galveston Bay	32
Figure 12 Cross Section of the Highland Bayou Incised-Valley and the Eastern Halls Bayou Incised-Valley	34
Figure 13 Cross Section of the Chocolate Bayou and Western Halls Bayou Incised-Valley ..	36
Figure 14 Interpreted Path of West Galveston Bay Incised-Valleys	37
Figure 15 Core/SBP of Terramar Beach	38
Figure 16 Core Descriptions of Terramar Beach, Indian Beach Bayou, and SLP 27	39
Figure 17 SBP of Echert Bayou and Jamaica Beach.....	40
Figure 18 SBP and Core Photo of WGB3.....	43
Figure 19 The Ideal Stratigraphic Column of West Galveston Bay.....	46
Figure 20 Core Descriptions of Galveston Island Cores	48

Figure 21 The Pleistocene Unconformity surface and the Paleo-Brazos River surface distribution	54
Figure 22 Interpreted Path of PBR.....	56
Figure 23 Geomorphic Features of Galveston Island	57
Figure 24 Interpreted Path of the Incised-Valleys beneath Galveston Island	61
Figure 25 Cross-Section from Follets Island to Bolivar Peninsula.....	62
Figure 26 Sea Level Curve.....	63

1. INTRODUCTION

Barrier islands are complex coastal systems covering 6.5% of the global coastline and 80% of the Texas Coastline (Brantley et al, 2014). Modern barrier islands and barrier spits protect back-barrier lagoons, bays and their associated ecosystems, acting as a shield from the brunt force of storms (Morton, 1994; Stutz and Pilkey, 2001). All of the world's modern barrier islands and associated back-barrier lagoons formed during the Holocene (Davis, 1994), mostly in the past 5,000 years, concomitant with the deceleration of the eustatic sea level rise (Davis and FitzGerald, 2009). Most barrier islands and back-barrier lagoons form on meso to micro-tidal, wave dominated coasts under a balance of sea level rise, sediment supply, coastal gradient, and wave energy (Carter and Woodroffe, 1994; Davis and FitzGerald, 2009). Consequently, barrier islands can be complex and contain antecedent geological features, such as beach ridges, healed storm surge channels, wided spits, and other coastal morphological features (Davis and Fitzgerald, 2009). In addition, barrier islands typically form atop relict Pleistocene and Holocene deposits. The surfaces of these deposits contain antecedent topography which may contain both simple and compound incised-valleys as well as storm surge channels, which may also extend under the back-barrier lagoons (Davis and Fitzgerald, 2009, McNinch, 2004).

According to Zaitlin et al, 1994, there are two types of incised-valleys that form due to lowering sea level; Piedmont incised-valleys, which are incised-valley systems with headwaters in a (mountainous) hinterland and cross a "fall line", and Coastal-Plain incised-valley systems, which are incised-valleys that are localized within a low gradient coastal plain and do not cross a "fall line". An incised-valley system that is filled during one depositional sequence is called a simple fill, whereas, if it is filled over multiple cycles of incision and deposition, it is called a compound fill (Zaitlin et al, 1994). Both the Brazos and Trinity Rivers have large drainage

basins that extend inland beyond the coastal plain, above the “fall line”. They have been active across multiple glacial cycles and contain fluvial terraces (Anderson et al, 2004, Anderson et al, 2014, Blum et al, 1995), but using Zaitlin et al (1994) classification, both are categorized as a compound piedmont incised-valley. The other modern drainage basins of West Galveston Bay (WGB), discussed in detail below, are Chocolate Bayou, Halls Bayou, Carancahua Lake, and Highland Bayou. Chocolate Bayou is the largest of the modern WGB drainage basins with an area of 227 km² and extends 42 km inland from the mouth. The other drainage basins are smaller and do not extend as far inland, but lie within the coastal plain and along with Chocolate Bayou, are classified as coastal-plain incised-valleys. Further investigation, included in this study, will be required to determine if they are simple or compound filled incised-valleys.

The upper Texas coast consists of a late Pleistocene coastal plain containing an antecedent topography, which includes both simple incised-valley systems as well as compound incised-valley systems containing fluvial terraces formed during the last sea level lowstand (Blum et al, 2001). This complex antecedent topography is overlain by Holocene deposits filling much of the incised-valley systems and forming barrier islands and deltas as well as filling in back-barrier lagoons (Blum and Aslan, 2006). These drowned valley systems act as sediment traps, preserving the Holocene stratigraphic record deposited during rising sea level and shoreline transgression (Anderson et al, 2014, Dalrymple et al, 1994, Rodriguez et al, 2004, Simms et al, 2006). Investigating the subsurface for the incised-valley systems along coastlines is essential for identifying sequence boundaries and recognizing how coastal environments respond to fluctuating sea levels (Blum and Törnqvist, 2000; Dalrymple et al, 1994). The sequence boundary is represented as the base of the valley, formed as an erosional feature, marking the beginning of valley incision (Dalrymple, 1994). These valleys can sometimes provide the only

record of marine transgression by providing accommodation space for the preservation of Holocene strata. This preserved strata and associated valley geometry can be studied to determine how the antecedent surface has influenced the distribution of sediment during barrier island and back-barrier lagoon formation.

Although the antecedent topography has been identified in a few cases as being significant in how barrier islands form (e.g. Belknap and Kraft, 1985; Oertel, 1985; Schwab et al., 2000), it is still understudied and poorly understood. How the antecedent geology affects the morphology of the islands and back-barrier lagoons are even less understood. Estuaries forming above incised-valleys are common along coastlines created by marine transgression; these estuarine systems are represented in the stratigraphic record but have not been widely recognized (Dalrymple et al, 1992).

The primary goal of this study was to determine if the topography of the Pleistocene surface influenced the geomorphic features and evolution of Galveston Island and WGB. This was accomplished by investigating the distribution of the incised-valleys through the barrier shoreline of WGB, the changes in island width and the presence of bay-side shoreline embayments and storm surge channels (**Fig. 1**). Some of the questions that needed to be answered were: Incised-Valleys were found on the most western sections of WGB (Lavery, 2014), is there a network of incised-valleys on the eastern side of WGB, if so what type are they? Did the placement of these incised-valleys have any influence on the geomorphology or formation of Galveston Island? How far did the paleo-Brazos River delta extend into WGB? To address this topic, this thesis tests the hypothesis: Topographic variations of the antecedent Pleistocene surface of the WGB system was a major control during the formation and evolution of Galveston Island. The hypothesis was tested by using high-resolution CHIRP seismic data to map out the Pleistocene

surface and identify any significant features in the antecedent geology (buried, incised-valleys) beneath WGB. Using geophysical data to interpret stratigraphy is a well-established method used in similar studies in the Galveston Bay area (Anderson et al, 2008, Lavery, 2014, Rodriguez et al, 2005). Identifying the antecedent topography (Pleistocene unconformity, seismic facies, subaqueous boundary conditions) was the first step in establishing the main control for the Holocene sediment distribution.

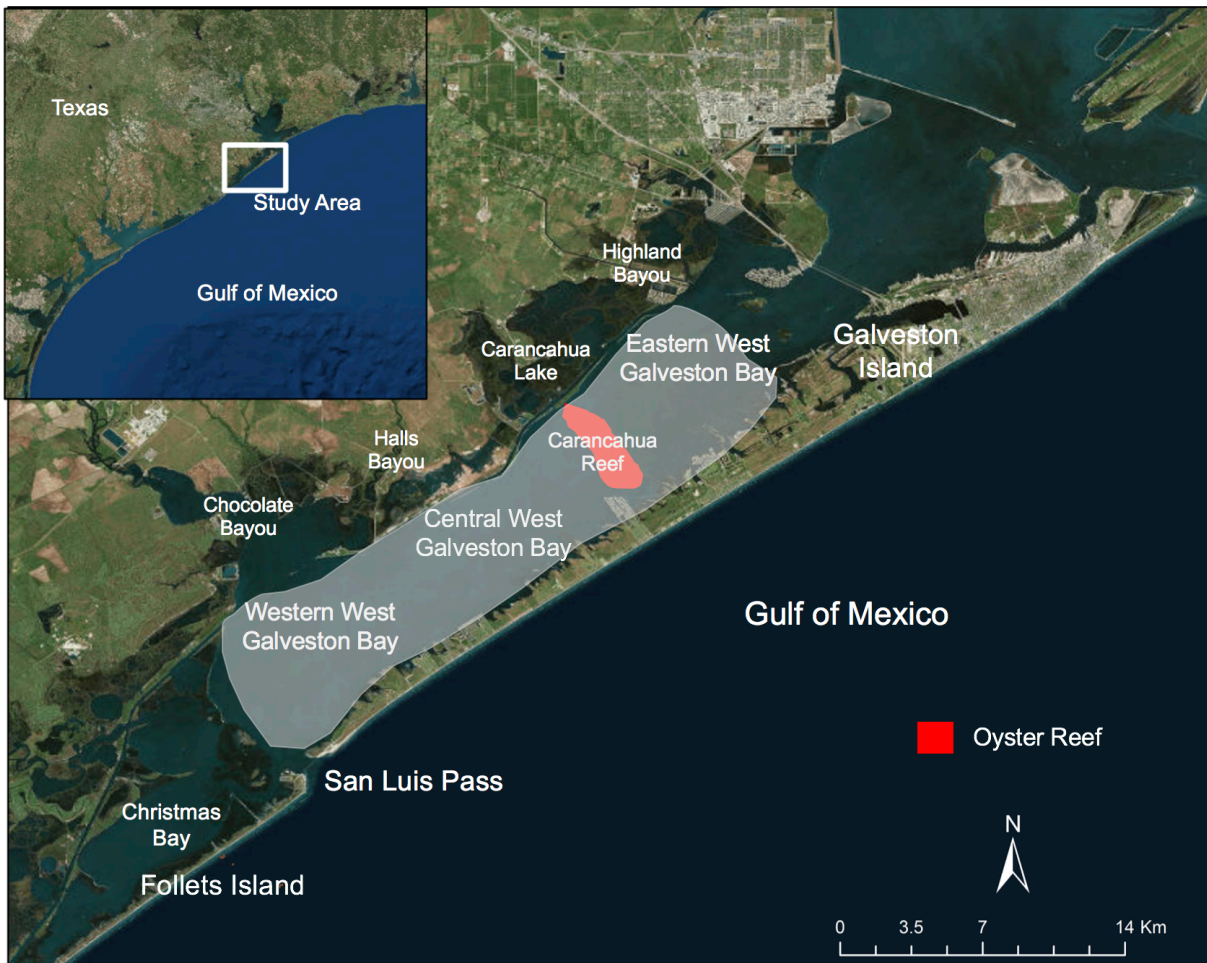


Figure 1. Regional Map. Maps showing the regional and local locations of the study area. The survey area is highlighted in grey.

Sediment cores were collected to sample the Holocene and Pleistocene sediment within WGB and Galveston Island to verify the geophysical interpretations as well as capture the transitions of the phases of island formation. The sediment samples were used to measure geotechnical parameters, including grain size distribution, compressive strength, and shear strength, which can determine how erosion and stress can affect the sediment. Collecting the sediment cores to sample the Pleistocene was more difficult than anticipated due to the dense Pleistocene subsurface precluding core barrel penetration and recovery of sediment from below the Pleistocene unconformity. These issues were addressed by using cores previously collected within WGB to review and evaluate evidence of the Pleistocene sediment.

To assess the role the antecedent features potentially played in the evolution/formation of the island shoreline, surficial geomorphic features of Galveston Island associated with the pathways of the incised-valleys were documented. The surficial geomorphic features included storm surge channels, overwash sites, and large coves extending into the island. For each geomorphic feature, the width, length, and proximity to the valleys were measured and variations in their sizes were used to detect how paleo-channels/valleys influenced the development of Galveston Island. Overall, the main objective of this study was to observe any links between the buried incised-valley systems and geomorphology of Galveston Island by integrating the findings from the geophysical interpretations and geomorphic observations. This project also investigated the presence of the paleo-Brazos River and mapped the extent of the river delta deposits using geophysical and sediment core data. Although the dispersal of the paleo-Brazos River is ancillary to this study, it is included because it was observed, and this study provides a venue to report these observations.

The phases of formation of Galveston Island have been documented in Wallace et al (2010) and Anderson (2007). If these phases correlate to the location of the buried incised-valleys, then the larger geomorphic features of Galveston Island were likely influenced by the antecedent topography beneath the island. Understanding these effects and influences could provide a better predictive tool for understanding future barrier island stability, the ability to predict locations of erosional hotspots and guide bay shoreline restoration efforts and shoreline protection. It also contributes towards a greater understanding of the geological controls on barrier island and back-barrier lagoon formation and evolution.

2. BACKGROUND

2.1 Barrier Islands and Back-Barrier Systems

Modern barrier island and estuarine systems are young geomorphic features, portraying the energetic depositional environment of the coast. Barrier islands generally form parallel to a low gradient coastal plain, separating the mainland from the ocean by a bay or lagoon (Davis and Fitzgerald, 2009). All modern barrier islands and associated back-barrier lagoons were established during the Holocene Epoch, which began ~11,700 years Before Present 1950 AD (yBP) (Davis, 1994) and most modern barrier islands formed in the past 5,000 years, when the rate of Holocene Sea Level Rise (SLR) decelerated (Anderson, 2007, Davis and Fitzgerald, 2009). A barrier island is formed by a combination of dynamic processes; abundant sediment, relatively steady rate of sea level, active wave and tidal processes, and a suitable geomorphic setting, each has a critical role in the initial formation and accretion of the developing coastal sand bar (Davis, 1994). The initial formation is heavily dependent on the regional tidal and wave processes, which affect the size and shape of the newly formed island followed by the availability of sediment. When the sediment supply is exhausted, the island transitions from an accretionary phase to erosional. Galveston Island is a large barrier island, protecting the mainland and blocking beach to bay sediment transport, but is currently is eroding from an exhausted sediment supply and an increasing sea level rise rate (Wallace et al, 2010). Because of short and long-term variations of these factors, barrier islands and back-barrier lagoons are in a constant state of flux (Houser et al, 2008).

Barrier islands protect estuaries from the marine environment by allowing limited access to oceanic processes and hindering sediment transport (**Fig. 2**). Estuaries are unique, complex depositional systems heavily influenced by both fluvial and marine processes which transport

sediment within the estuary. Estuaries can be geologically unstable due to their formation being heavily regulated by sea level fluctuations, wave and tidal processes, and sediment supply (Perrillo, 1995). It is common for estuaries to form above the most seaward portion of drowned channels systems along transgressive coasts with the deposited sediment being preserved within the abandoned channels (Dalrymple et al, 1992). Investigating barrier islands and their associated lagoons can provide a better understanding of the inter-relationship between antecedent geology and lagoon/island evolution.

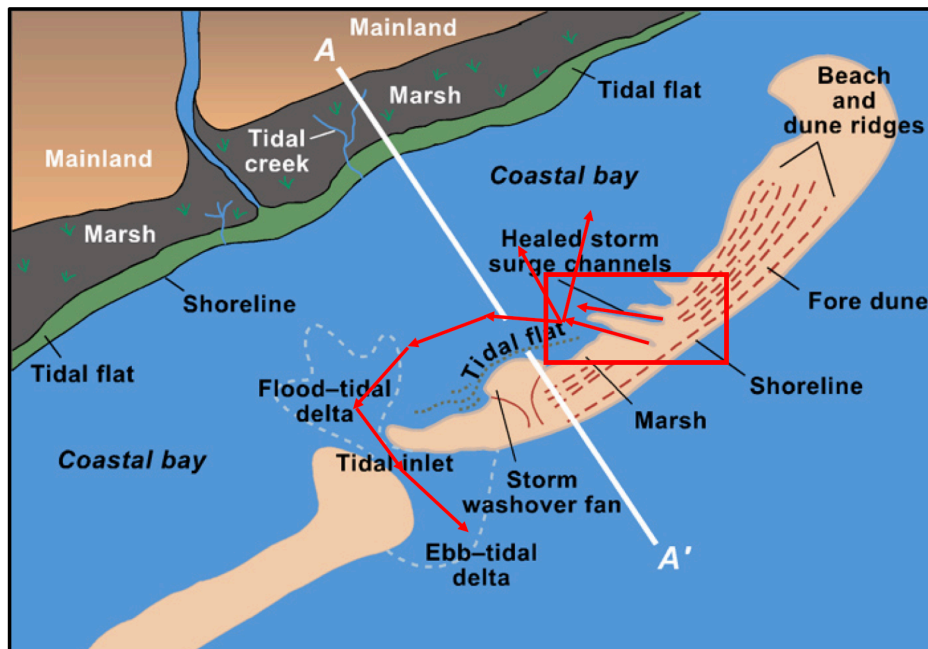


Figure 2. The Barrier Island System. The storm surge channel on the bay shoreline are highlighted in red with arrows showing the ebb and flow of the storm surge. (Modified from Bureau of Economic Geology (n.d.)

Storm surge channels, also called hurricane channels, are channels that have cut through the backshore of barrier islands (**Fig. 2**). These channels are initially incised by the ebb and flow of storm surge flooding during and after a tropical storm. During a pre-frontal passage of the storm, overwash on the island creates channels and overwash fan deposits. After the passage of

the storm front, the storm surge ebbs out of the bay, enhancing the channel through erosion and transporting sediment towards the ocean, creating a washout deposit in the back-barrier lagoon (Hayes, 1966; Morton, 2002). On the bay-side, evidence of the channels can persist or never fully recover, as evidenced by numerous relict storm surge channels along the bay shorelines of the barrier islands of Texas that are easily observed from aerial photographs (**Fig. 3**). This weakness in the island structure is due to the channel being filled with sediment within the relict channels that is less consolidated than the surrounding sediment, making the channel fill less resistant to future erosion during the next storm. Storm surge channels are abundant along the bay-side of Galveston Island, connecting the island to the back-barrier lagoon and are reactivated during extreme flooding and storm events (Rodrigues et al, 2001), and may contain a depositional record of these events. However, along most of west Galveston Island, these channels ceased to be active around 3,000 yBP, when the island achieved a critical width that prevented overwash (Morton, 1974).

2.2 History of Transgression in Texas

Since the Last Glacial Maximum (LGM), 22,000 years ago, the upper Texas coast has experienced numerous environmental changes caused by recurrent sea level fluctuation acting as a major control on the development of modern coastal morphology (Anderson, 2007; Davis, 1994). The last sea level lowstand occurred 18,000-15,000 yBP, when global temperatures were lower and precipitation was greater (Flint, 1957, Schumm, 1965, Hays et al, 1976). A transition initiated by increasing temperature and decreasing polar ice sheets caused the eustatic sea level rate to rise rapidly, forcing shorelines to migrate landward (Anderson et al, 2004). This event instigated the first stage of marine transgression along the Texas coast. Around 7,700 yBP, a

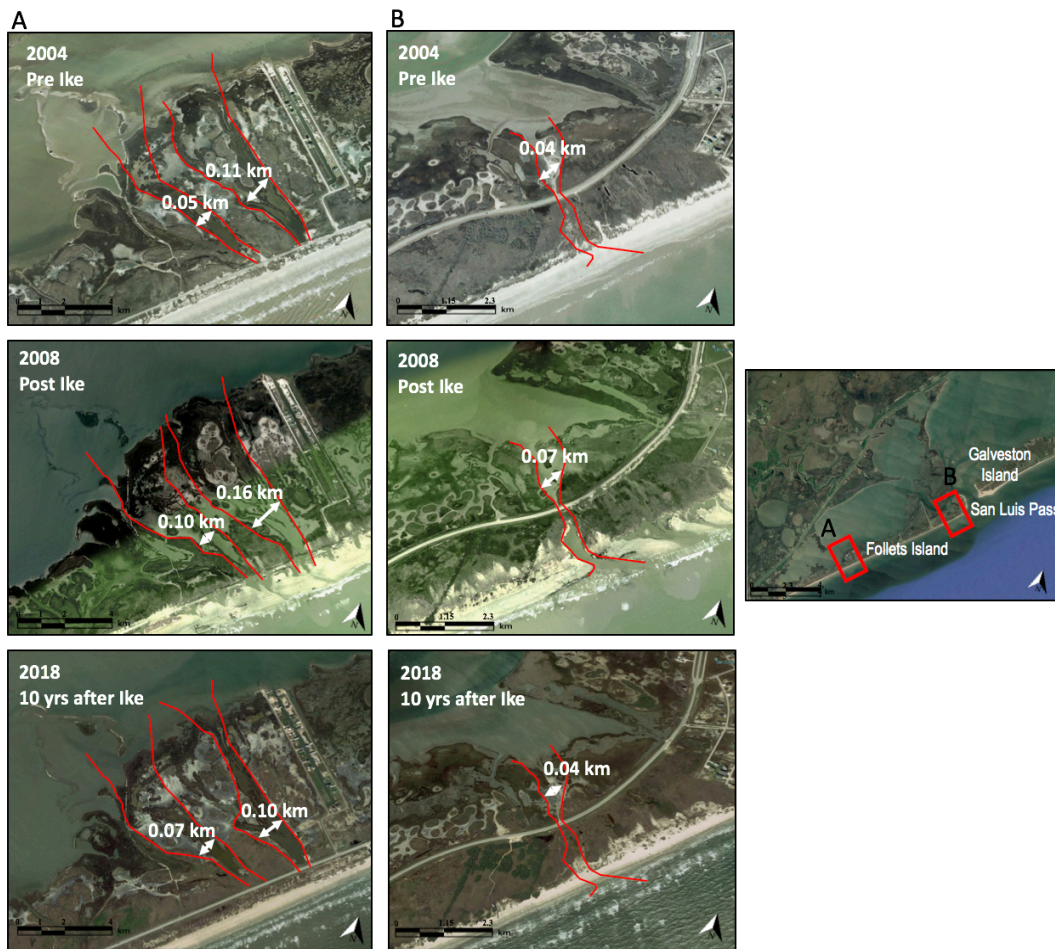


Figure 3. Formation and Preservation of Storm Surge Channels. A and B are a time series showing the formation and preservation of Storm Surge Channels and breach sites of Follets Island from 2004-2018. 2004- Open and active bay-side storm surge channel. 2008- Post-Ike. Storm Surge of Hurricane Ike; the channel was opened on the ocean-side, breaching the island and created open transport between the ocean and bay, road acted as obstacle. 2018- 10 years after last breach event. The beach side has healed and closed the ocean side breach. Storm surge channel is still open on the bay-side.

flooding event accelerated transgression, causing the shoreline to migrate landward, and coincides with the first evidence of estuarine deposits appearing in the incised-valleys of WGB, indicating the beginning of inundation (Lavery, 2014; Rodriguez et al, 2004). The next flooding event occurred 5,500 yBP, when the rate of sea level rise decreased from 2 mm/yr to 0.4 mm/yr (Milliken et al, 2008). An abundant sediment supply and steady sea level rate enabled a barrier

island to form atop the Pleistocene surface while fluvial deposits were diverted to accumulate in present-day WGB. At 4,400 yBP, a final flooding event occurred, moving the shoreline close to its present-day location. The presence of incised-valleys allowed space for sediment to be deposited at sea level and the sedimentary environment has remained steady, while Galveston Island began to form to its current state (Anderson et al, 2004). Modern Holocene estuaries develop above low topographic valley systems with the size depending on the width of the channel/valley and location of fluvial terraces by influencing the rate of sedimentation. Knowing the location of the incised-valley features can be helpful in understanding the formation of an estuary.

The formation of WGB has been discussed in previous studies (Bernard et al, 1970; Taha and Anderson, 2007), but a recent study by Lavery (2014) reconstructed the Holocene paleoenvironment of the western end of WGB. The data and interpretations from this study helped develop the framework for this project. Lavery (2014) found a small network of Pleistocene incised-valleys below the modern estuary, which formed during the sea level lowstand and were flooded by eustatic sea level rise ~9,000 yBP, subsequently filling the channels with Holocene sediment. Lavery (2014) found the channels to be filled with a fluvial/estuarine stratigraphic succession controlled by flooding events and fluctuating sediment supply. Included in this succession was the record of the ancestral Paleo-Brazos River (PBR) delta between 6,100-4,000 yBP, before the PBR migrated south and emptied further down the coast (Bartek et al, 1990, Lavery, 2014, Rodriguez et al, 2004). The episodic flooding of WGB transitioned the depositional environments from paleo-bayhead delta to modern estuary by trapping sediment within the channels over a 9,000 year to present-day period (Wallace et al, 2009). The 4,400 yBP flooding event was the final step in fully inundating the present-day

estuary of WGB. Even though the area was inundated, it did not reach its modern shape until it was semi-enclosed by the modern western tip of Galveston Island around 1,800 yBP. The present-day WGB was fully established as an estuary around 1,500 yBP, sitting above a system of abandoned river channels filled with Holocene estuarine and fluvial deposits sourced from inland distributaries and marine sediment.

During fluctuating sea levels throughout the Quaternary period (2.6 mya-present), a series of geological formations were deposited along the Texas coast, the Beaumont and the Deweyville formations. The Deweyville Formation along the Neches and Sabine Rivers of East Texas was identified by Bernard (1950) and represents Quaternary aged, unconsolidated, sand deposits of a variety of colors; gray, brown, or blue-gray (Blum et al, 1995). The Deweyville sediments were deposited during Glacial Stage 3 (57-29 kya) when the sea level was lower than present-day MSL, leaving behind traces of a fluvial delta and fluvial terraces (discussed further below). The Beaumont Formation formed during the sea level highstand (6 m above MSL) and represents Glacial Stage 5e (124-119 kya) deposition, the last interglacial period before the Holocene (11 kya-present) (Blum et al, 1998). It has been extensively studied along the upper Texas Coast within the Sabine and Trinity River Incised-Valleys (Blum et al 1995; Garcia, 1991). The Beaumont Formation is the most recent mass deposition of fluvial delta sediment found in shallow depths on the subsurface and is younger than the Deweyville Formation (Garcia, 1991). Sediment from this formation is a hard, consolidated, inundated paleosol of various colors.

2.3 Incised-Valleys

Before and during the LGM (22 kya), the coastal plain along the present-day coastline of the Gulf of Mexico (GOM) contained a series of incised-valley systems, formed during the falling stage of sea level, extending across the continental shelf (Blum and Aslan, 2006). As noted previously, there are two types of incised-valleys: (i) piedmont incised-valleys, which are large valley systems fed by large drainage basins; and (ii) coastal-plain incised-valleys that are formed by small, coastal plain rivers with typically small drainage basins, creating a smaller valley system. The large estuarine systems along the Texas coast are formed within compound piedmont incised-valleys and generally contain both Pleistocene fluvial terraces (Anderson et al, 2008; 2016) as well as Holocene fluvial/estuarine fill (Simms et al, 2006). In addition, there are simple, coastal-plain incised-valleys contained within these estuaries, created by smaller coastal-plain rivers that exist along the banks of the large estuarine systems (Lavery, 2014). The locations of incised-valleys tend to be in lower lying topography due to transgressive erosion removing earlier subaerially exposed surfaces, which make the valleys susceptible to inundation during the transition to sea level rise (Lavery, 2014; Posamentier and Allen, 1993). Once relative sea level begins to rise, incision ends and the coastal depressions gradually fill with sediment, drowning the incised-valleys by repeated flooding events (Gibling, 2006; Posamentier and Allen, 1993). The stratigraphy preserved within an incised-valley is dependent on the depth of incision and the rate of sediment deposition (Dalrymple et al, 1994). Studying the preserved sequence stratigraphy within incised-valleys can provide a glimpse at the paleo-environment of the present-day coastlines.

As noted above, along the Texas coast, the piedmont incised-valleys contain fluvial terraces (**Fig. 4**). The terraces are well-preserved accretional ridges formed by the downcutting

of sea level during a falling stage (Nordfjord et al, 2005). They were created by different periods of incision and can be used to establish a time frame of valley incision (**Fig. 4**) (Anderson et al, 2004). The presence of terraces can provide accommodation space for sedimentation, be a precursor to estuary formation, enhance subsidence, create estuary widening, and heavily influence coastal environments during SLR and flooding events (Nordfjord et al, 2005; Rodriguez et al, 2005). Beaumont and Deweyville terraces contain the Beaumont and Deweyville formations, respectively, and are present along the Trinity River Incised-Valley walls beneath modern-day Galveston Bay. The Deweyville terrace morphology occurs at two elevations; -10 m and -14 m, as the High and Middle Deweyville terraces, formed during the Glacial Stages 3 (57-29 kya) and 4 (71-57 kya), respectively (Blum et al, 1995; Rodriguez et al, 2005). During the Holocene transgression, each terrace became inundated by a major flooding event at 7,700 and 8,200 yBP (Rodriguez et al, 2005). The Beaumont terrace occurs at elevations higher than the High Deweyville terrace, was deposited at Glacial Stage 5e (124-119 kya) and earlier. It was the most recent fluvial terrace in the Trinity River Incised-Valley that was flooded by the rising sea level. The presence of terraces can play a role in the response of coastal sedimentary environments to rising sea level as well as pinpoint stratigraphic sequences.

The shape of the valley and channel is significant to how the estuarine sediment is distributed, especially during the initial flooding periods, and how the estuary evolves during the Holocene transgression (Dalrymple et al, 1992). Studying and mapping incised-valleys provides a detailed opportunity to look at the flooding events and depositional environments of a specific area and time frame. The networks of incised-valleys within WGB were created by a large paleo-river, or its distributary streams, eroding and transporting Pleistocene sediment to the continental shelf during a decrease in eustatic sea level. Once sea level began to rise, Holocene sediment was

distributed and deposited to fill the paleo-valleys with the distribution of the sediment being heavily influenced by the incised-valleys themselves. The Chocolate and Western Halls Bayou Incised-Valleys were first identified in Lavery (2014). It should be noted that Lavery (2014) used the classification of “incised channels” for what is classified in this study as coastal-plain incised-valleys. These incised-valleys were reinterpreted for this project in more detail using the raw seismic data collected by Lavery (2014) and renamed, following the new nomenclature. Lavery (2014) concluded that these coastal-plain incised-valleys were active before 9,000 yBP, based on the calculated sea level curve and the depth of the base of the valleys. Lavery (2014) also states that Chocolate Bayou was occupied by the Brazos River as part of an ancestral Paleo-Brazos River delta. Both valleys mapped by Lavery (2014), the CBIV and WHBIV, were reinterpreted in this study to further delineate the Pleistocene Unconformity and the channel geometry as well as any connections to other buried channels within WGB.

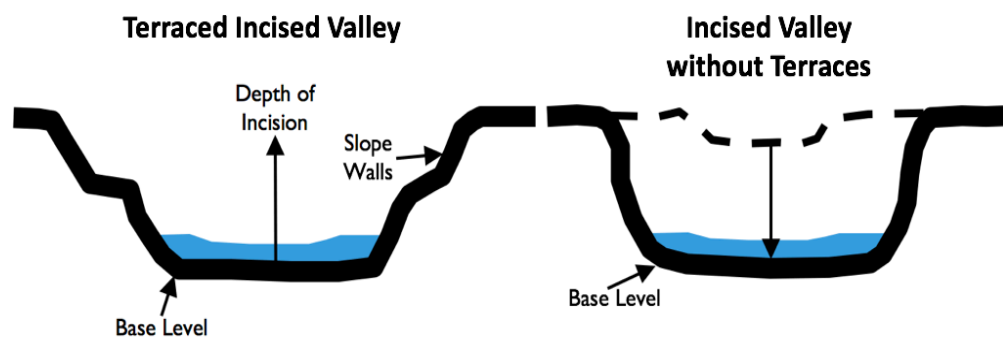


Figure 4. Types of Incision. They different types occur from river floodplain and sea level rise.

2.4 Pleistocene Unconformity in West Galveston Bay

Across the coastal plain and continental shelf of Texas, the Beaumont Formation, also known as the Beaumont Clay, forms the upper Pleistocene stratigraphic interval, the surface of which is marked by the Pleistocene Unconformity (PU). The Beaumont Formation was

originally deposited as a fluvial clay but was exposed during the Pleistocene lowstand and the upper portion of the Beaumont Formation became a paleosol, consisting regionally of inundated, hard, dense, clays and sand, containing an abundance of carbonate concretions, and is typically red, green, orange or white in color (Garcia, 1991; Rodriguez et al, 2005) (**Fig. 5a**). It is generally so hard and dense, that only a few centimeters to decimeters at most can be recovered in a vibracore. The PU can be easily identified in seismic data, where it is demarcated as a dark, high acoustic impedance seismic reflector, indicating a hard surface. Within WGB, the Pleistocene strata is interpreted as continuous, sub-parallel, high amplitude reflectors (**Fig. 5b and Fig. 5c**). Within the western portion of WGB, the mapped surface of the Pleistocene reveals a fluvial terrace cut by two incised-valleys, named the Chocolate Bayou and Halls Bayou Incised-Valleys, named after the present-day fluvial systems from which they appear to extend.

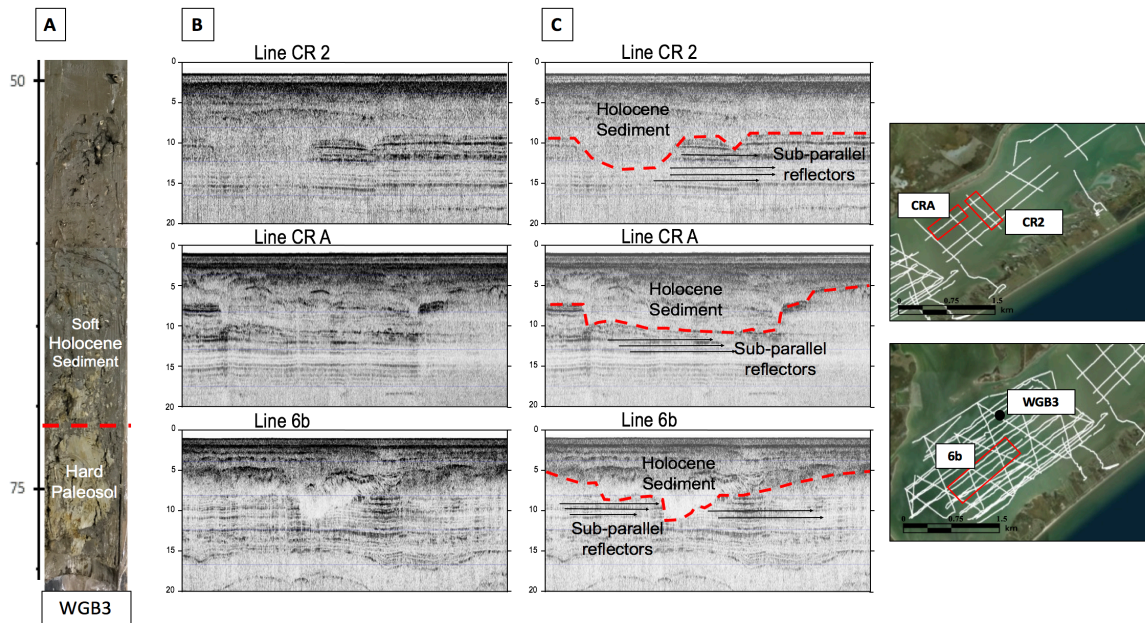


Figure 5. Evidence of Pleistocene Unconformity. A. Image of WGB3 with the Holocene to Pleistocene transition (red dashed line). The greenish clay is the surface of the Beaumont Formation. B. Uninterpreted seismic images of Lines CR2, CRA, and 6b. C. Interpreted seismic lines showing the Pleistocene Unconformity in West Galveston Bay.

The mapped incised-valleys extends from the northern shore of WGB, across WGB to the northern shore of Galveston Island. Lavery (2014) found that these valleys are incised into the Pleistocene strata, making them Pleistocene in age, and filled with Holocene strata.

2.5 Holocene Stratigraphic Sequence

The stratigraphy of the western side of WGB contains sediment from many depositional environments; fluvial/deltaic to estuary and marine, each change being initiated by flooding intervals at 9,000 yBP, 7,600 yBP, 6,800 yBP, and 4,400 yBP (Lavery, 2014). The flooding events redistributed the sediment, thus changing the depositional environment, with the final event around 4,400 yBP inundating WGB. The findings allowed a preliminary view of the formation of the incised-valleys below low-lying estuaries and the Holocene stratigraphic succession of WGB. This project extended Lavery's (2014) study of the eastern side of WGB, focused at a different perspective and utilizing the characteristics from Lavery (2014) to interpret the Pleistocene sequence boundary. The Holocene sediment can be easily distinguishable from the Pleistocene sediment. The Holocene is soft mud deposited within the last 12,000 years, while the Pleistocene is an older, harder sediment, deposited from 2.4 million-12,000 years ago. The Pleistocene sediment in the upper Texas coast has experienced subaerial erosion, sea level fluctuation, and, in some places, river scouring. The upper Pleistocene strata is typically a paleosol, oxidized and/or leached as part of the development of a soil profile (Bernard et al, 1962). The Holocene and Pleistocene strata differ in terms of their grain size composition and geotechnical properties due to the Pleistocene sediments being more cohesive than Holocene mud (Wallace et al, 2009), suggesting a higher overall clay content. The typical shear strength of the Holocene sediment is 0.05-0.1 kg cm⁻² (Rodriguez et al, 2001), whereas the Pleistocene

sediment typically has a shear strength $>1.0 \text{ kg cm}^{-2}$. The Pleistocene strata has an order of magnitude lower shear strength due to the consolidated clay hardened by frequent exposure and induration. Its relatively high shear strength and hard composition makes it difficult to penetrate and sample. It also demonstrates that the Pleistocene strata is well compacted, meaning it can bear a greater load without additional compaction and is extremely resistant to erosion. For the Holocene, sediment compaction has been the dominant process contributing the subsidence and coastal erosion.

2.6 Analyses of Bay Shoreline Retreat

One way to determine if the presence of the incised-valleys influenced the formation of Galveston Island is to compare the retreating/advancing rates of the bay shoreline along proximal sections of the island both underlain by incised-valleys and sections without. Based off an analysis of the change in bay shoreline position from the Texas Department of Economic Geology, this report shows long-term rates in shoreline change along the bay shoreline of the WGB system including WGB, Drum Bay, Christmas Bay, Chocolate Bay, and Halls Lake. The historical positions of the historical shorelines are combined in a linear regression model to estimate an average annual rate of bay shoreline change. The bay shoreline change rate at Carancahua Cove, where HBIV is located, range from -3.4 to -13.7 m/yr, one of the highest retreating areas of Galveston Island (**Fig. 6**) The shoreline change rates in the surrounding areas, Jamaica Beach and Dana Cove, have smaller retreating rates (-0.4 to -1.0 m/yr) or are advancing (0.1 to 0.4 m/yr) (Gibeaut et al, 2003). Along the CWGB shoreline, the incised-valleys split and extend beneath two sections of the island with depths of -10 to -12 m with the shallowest being -5 to -7 m under the island. For CIV/EHBIV, Maggie's Cove and Bird Island Cove have a

localized bay shoreline change rate of -0.4 to -13.7 m/yr (Gibeaut et al, 2003). The surrounding areas are Ostermayer Bayou (-0.2 to 0.6 m/yr) and Snake Island Cove (-0.2 to -8.9 m/yr). Snake Island Cove is a large embayment similar to Maggies and Bird Island Cove but is retreating at a lower rate. Along the back-bay shoreline on the west end, there exists an unnamed marsh embayment above the CBIV/WHBIV. The merged valley is -10 to -12 m deep, Holocene filled and extends under the island (**Fig. 6**). The embayment has a bay shoreline change rate of -3 to -10 m/yr above the location of the incised-valley. The surrounding areas have a rate of 0 to -2.7 m/yr. (Gibeaut et al, 2003).

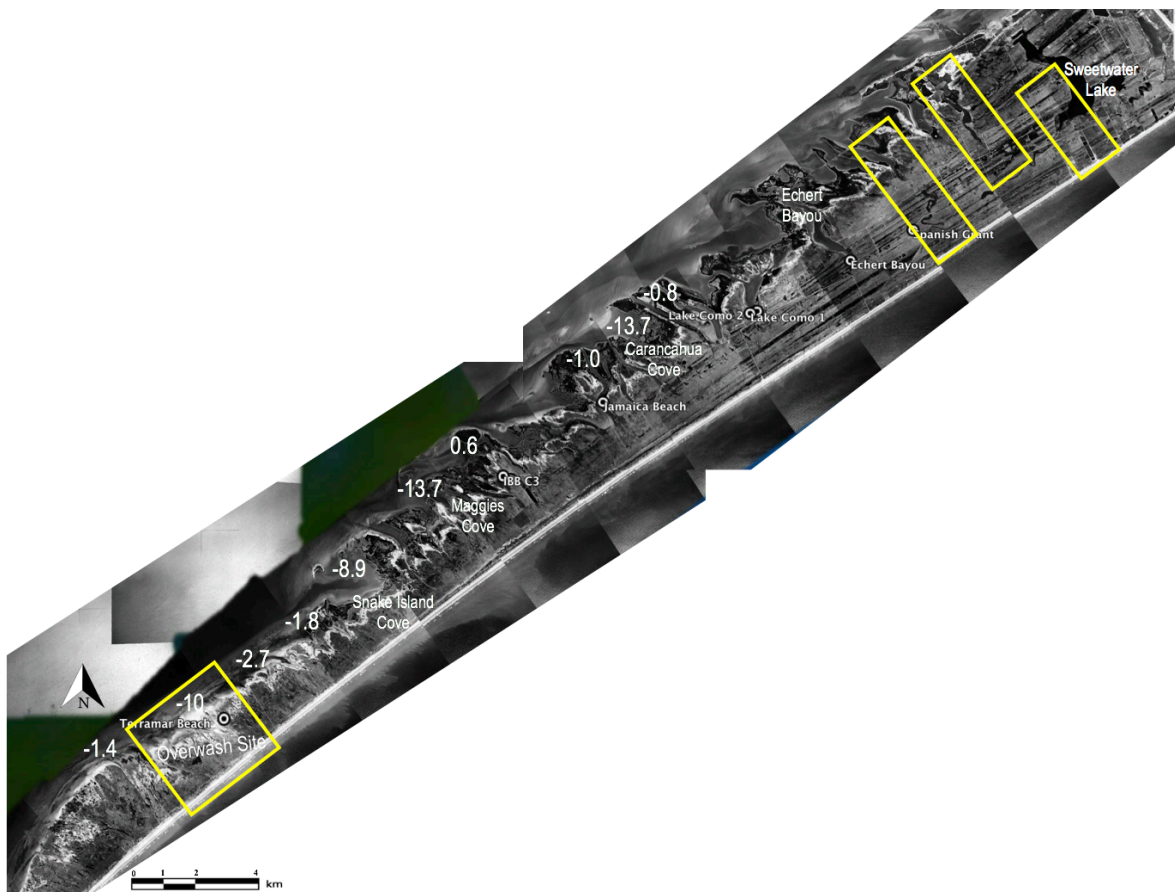


Figure 6. Breach Sites and Shoreline Erosion Rates Along the Bay Shoreline. Photo mosaic of 1954 from Google Earth. The numbers on the bay shoreline are rates of shoreline change (m/yr) (Gibeaut et al, 2003). The yellow boxes are breach sites, the ones near Sweetwater Lake are older and no longer breach across the island. The overwash site on the west end is more active, breaching during a major storm event.

3. STUDY AREA

3.1 Galveston Island

Galveston Island is located between Bolivar Peninsula and San Luis Pass on the upper Texas coast in the Northern Gulf of Mexico (Bernard et al, 1970). Between Galveston Island and the mainland sits WGB, a back-barrier lagoon (**Fig. 1**). According to Wallace (2010), the eastern 30 km of Galveston Island began forming approximately 5,500 yBP, contains a series of well-preserved beach ridges and swales, and is generally 5 km wide (**Fig. 7**). This section is the oldest and widest section of the island, making it the first phase of the islands formation. In contrast, the western 15 km of the island are generally less than 1.5 km wide and formed approximately 3,000 yBP when the sea level rate increased from 0.25 m/yr to 1.30 m/yr (Rodriguez et al, 2005).

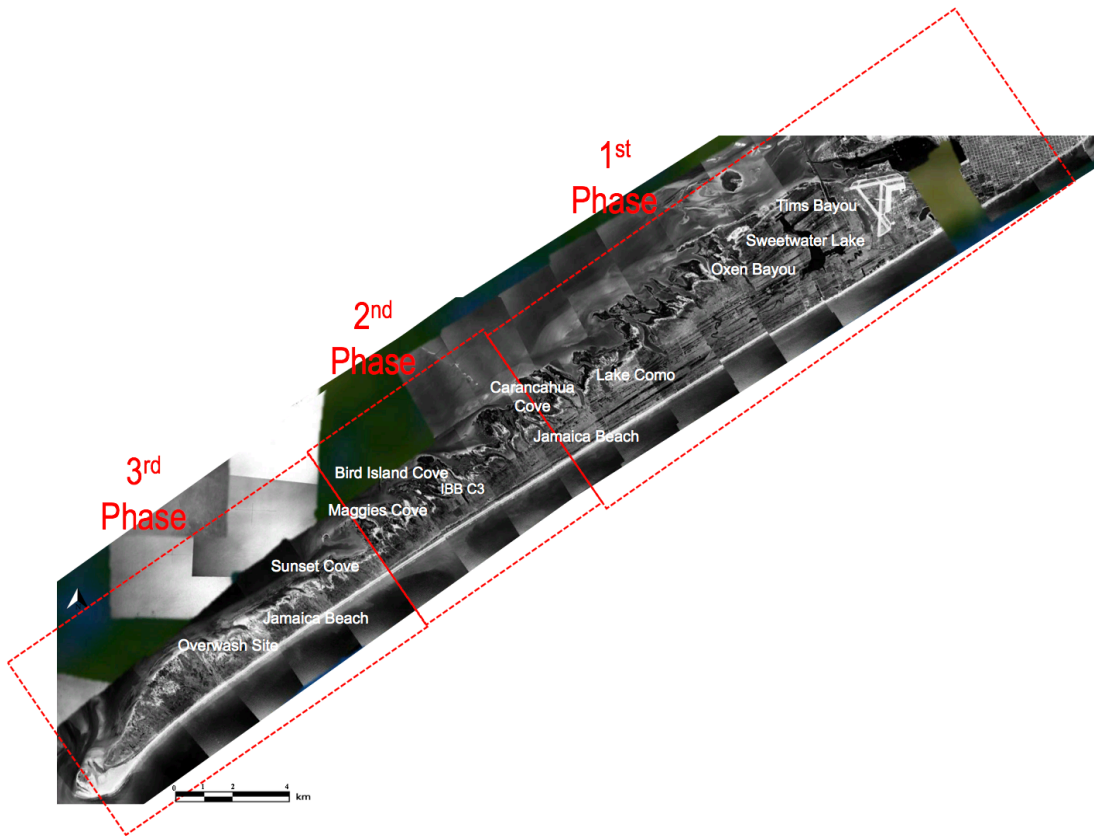


Figure 7. Phases of Island Formation. 1954 mosaic image with phase of barrier island formation and areas of interest.

This phase of formation can be divided into two parts, with the final phase ending the island accretion ~1,800-1,200 yBP due to an exhausted sediment supply and steady rate of sea level (Wallace and Anderson, 2013). Along much of the eastern end of Galveston Island, within WGB, the Pleistocene surface is generally uniformly flat and is generally 2-3 m below the subsurface. However, along the western end of WGB, the Pleistocene surface has a high degree of spatial heterogeneity making it much deeper in some areas, 11 m or more below the subsurface (Lavery, 2014). Sets of beach ridges extend approximately parallel to the shoreline and represent the depositional morphology of Galveston Island (Bernard et al, 1959), while the west end of the island is dominated by storm washover features.

3.2 West Galveston Bay

WGB is a back-barrier lagoon located on the bay-side of Galveston Island, commonly known as West Bay (**Fig. 1**). It formed above Brazos River deposits after the formation of Galveston Island, around 5,000 yBP (Bernard et al, 1970). WGB terminates to the west at San Luis Pass, a natural tidal inlet, separating Galveston Island from Follets Island. Christmas Bay is the back-barrier lagoon of Follets Island and is separated from WGB by a series of small islands extending north-south across the western shore of WGB. WGB is a low energy estuary containing fine grain sediment (<63 μm) delivered to the bay by inflow from Chocolate Bayou to the north, transported from Galveston Bay to the east and from inflow through San Luis Pass to the west. The tidal range is primarily diurnal with a daily range of ~30 cm (Wallace et al, 2009). WGB is divided into two sections by a narrow transverse oyster reef known as Carancahua Reef (Lavery, 2014). It is connected to Chocolate Bayou to the north via a dredged channel. Chocolate Bayou provides freshwater and fluvial sediment from four

tributaries, each with an incised-valley (Lavery, 2014). Taha and Anderson (2008) suggest that the incised-valleys are abandoned meanderbelts formed by the Brazos or Trinity River Incised-Valley system.

4. METHODS

4.1 Geophysical Survey

Over 90 km of new 2D high-resolution seismic sub-bottom profiles (SBP) were collected using an Edgetech® 216 Full Spectrum (CHIRP) seismic sonar towfish. This sub-bottom profiling system operates on a frequency range between 2 and 16 kHz. The CHIRP sonar is a quantitative acoustic measurement system used to determine the attenuation of coastal sediments and create a vertical sediment profile in real time. CHIRP is an acronym for Compressed High Intensity Radar Pulse and is used to describe the type of sound pulse used to generate the vertical profile of substrate. A topside computer controls the sound pulse through a source array and collects the pulse through a receiver array. The typical resolution for the Edgetech system is 0.05-0.1 m and penetration depth of 0-50 m. For this study, a resolution of 0.1 m and penetration of up to 35 m was achieved. The survey was collected using a narrowed frequency range between 12 to 15 kHz, depending on the composition of the subsurface to achieve optimal resolution of the rendered image and penetration of the sound pulse. The variable towfish layback was reduced by towing the towfish system alongside the GPS receiver, which has a 95-98% accuracy.

Over 200 km of high-resolution seismic data were used to interpret the subsurface features within WGB and Galveston Island. The other 110 km of the seismic data were collected in a previous study by Laverty (2014). The raw SEG-Y files from the project were collected using the same methods and processed with the new dataset for accurate file conversion and corrections. The survey was conducted on the R/V Rockport/Bateau owned by Texas A&M University Galveston Campus. The seismic lines were collected in a grid pattern within WGB and the canals of Galveston Island to maximize the line coverage (**Fig. 8**). Along much of the

western end of Galveston Island exists a series of bay-side canals, providing access to the bay. In most cases, these canals were dredged to less than 3 m below mean sea level (MSL). CHIRP surveys were conducted within all the major canals along Galveston Island, including the canals within the communities of Lafittes Cove, Jamaica Beach, Sea Isle, Sunset Cove, Terramar Beach, and Isla del Sol (**Fig. 8**). These canal surveys allow for the extension of open bay CHIRP lines into the interior of Galveston Island.

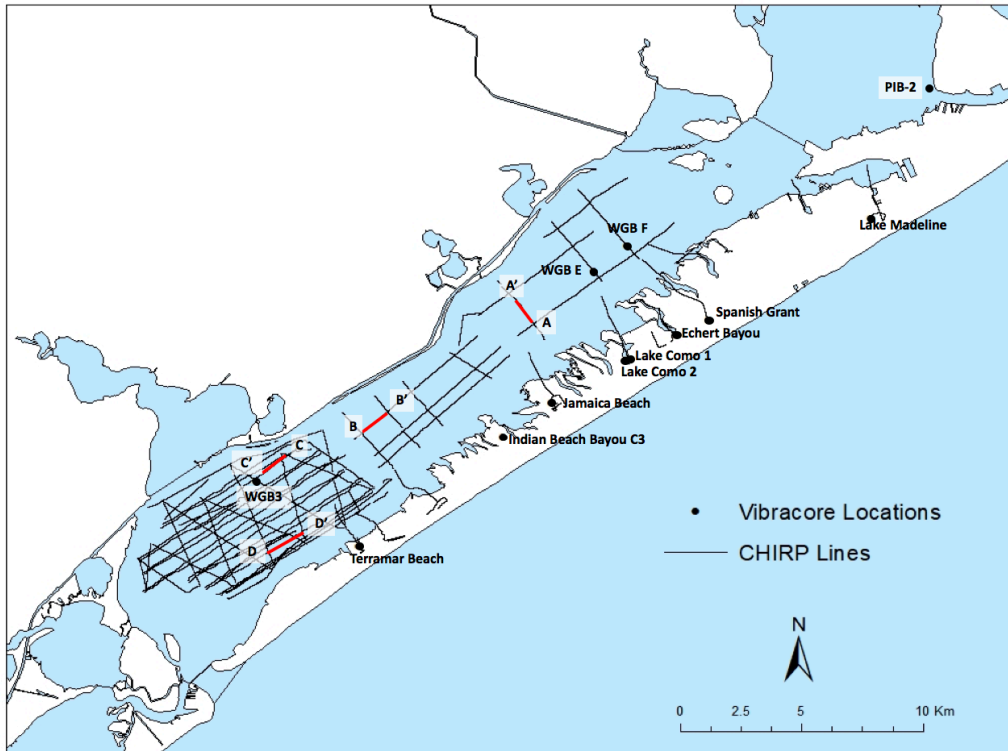


Figure 8. Core Location and Survey Map. Map of seismic survey, core locations, and canal communities on the bay side of Galveston Island. The seismic lines used for cross-sections are highlighted in red.

The seismic data was used to interpret the subsurface stratigraphy and accurately map the Pleistocene unconformity. The 2D high-resolution seismic data was processed and interpreted using Chesapeake® SonarWiz software. Each seismic line was picked for reflector horizons based on the changes in amplitude. Gain values for each individual section were adjusted to

enhance the resolution of the acoustic reflectors and reduce background noise and signal traces. Continuous reflectors were traced, and their depths were subsequently calculated using an assumed seismic velocity of 1500 m/s, based on previous studies (Anderson et al, 2004; Simms et al, 2010, Lavery, 2014). Surfaces were generated using the kriging interpolation tool in ArcMap. The Fence diagram was created using the horizon picks and Chesapeake® SonarWiz software. The area maps were created using Google Earth and ESRI® ArcGIS.

4.2 Sedimentary Analysis

A series of vibracores from 12 locations were collected within the Galveston Island neighborhood canals aboard the R/V Lithos (**Fig. 8**). The location of each core was selected based on the seismic sub-bottom data in order to recover Holocene and Pleistocene strata. The cores were collected using two types of coring techniques; an Oztec non-submersible and a PLV tech submersible vibracore system. The cores were between 0.8-3 m in length. Each core was photographed, visually described, and x-rayed within the Coastal Geology Lab at TAMUG. An additional series of 30 cores of various lengths, previously collected in WGB and processed using identical methods, were analyzed to observe the stratigraphy of the Holocene strata and verify the distribution of the Pleistocene and PBR.

Grain size distributions were determined from samples collected in 5 cm intervals. For each sample grain size distribution was determined using the Malvern Mastersizer 2000®, which uses laser diffraction to determine the grain size distribution of sand (62-2000 μm), silt (4-63 μm), and clay (0.1-4 μm). The grain size results and lithofacies interpretations were used to create a lithological description of each core. Issues with sediment recovery made it difficult to collect more cores within WGB. Cores from the Lavery (2014) study were re-examined to find

any correlation between the stratigraphy in WGB sediments. The lithofacies of the WGB area were correlated to the previous study using lithological descriptions and seismic data. The lithological descriptions were also correlated to the cores across Galveston Island. The shear strength, grain size, and visual descriptions were used to distinguish the Holocene and Pleistocene sediment within the cores collected.

Sediment samples from the Holocene and Pleistocene stratigraphic sequences were measured for shear strength using a Pocket Torvane Shear Test and compressive strength using a pocket penetrometer. These measurements are used for gauging the of sediment in the field or lab (Ameratunga et al, 2016). Samples were measured from the split core in intervals of 10 cm. For the Pocket Torvane Shear test, the vane size ratio was determined based on the consistency of the sediment. Vanes with a ratio of 0.2 and 1 were used for the soft mud and stiffer clays. The torvane was pushed into the sediment and the knob was turned counter-clockwise. A maximum shear value is measured when the spring tension fails. The shear value was then divided by the vane ratio to determine the shear strength of the sediment. Shear Strength is used to determine the sediments resistance to erosion. Compressive strength was measured with a pocket penetrometer by inserting a spring barrel into the sediment. If the sediment was a soft mud, an adapter foot (25mm) was added to the spring then the rod was pushed into the sediment to obtain a direct reading. This method measured the compressibility of the sediment, or how easily the sediment can be compacted. The amount of compressive strength is important to measure for this study to determine if differential compaction affects the sediment. Both methods are primarily used to gauge the cohesion of sediment, but can contain errors due to only measuring a small area of the sample. To mitigate any errors, multiple measurements were taken and the average was used in the results.

5. RESULTS

5.1 Seismic Results

A total of 92 km of new seismic lines were collected for this study within the eastern and central sections of WGB and through each of the major dredged canals, to extend the survey seaward as far as possible under the interior of the modern Galveston Island. An additional 110 km existing seismic data from within the western section of WGB, originally interpreted by Lavery (2014), were used to extend the study area to the western side of WGB. This combined dataset was used to make seismic interpretations of the antecedent geology within WGB. The seismic interpretations were based on the evidence presented in the data. Some of the interpretations were verified by sediment samples or knowledge from previous studies, but some were not verified due to insufficient sampling. Those interpretations are subjected to some speculation.

The CHIRP data from within the canals of west Galveston Island exhibited many erosional and depositional features. The canals contain a dredged subsurface to a depth of 0.2-1 m below MSL, and although they contain varying thickness of sediment fill above the dredged surface, it was easily identified as a thick, dark, irregular reflector below the subsurface, truncating generally horizontally bedded strata and verified in the sediment cores. Throughout the study area, the PU was easily identified in the CHIRP seismic lines as a dark reflector with erosional features and exists at depths ranging from 1-10 m below the dredged surface (**Fig. 9**). Below the dark reflector was a sequence of stratified sub-parallel reflectors of moderate to low amplitudes representing older Pleistocene strata.

The PU sequence boundary within the island has comparable characteristics to the PU on high topographic areas within WGB and was easily mapped, the only incised-valley interpreted

beneath Galveston Island was observed within the Jamaica Beach canal. In some of the narrower canals, the seismic data were difficult to interpret due to dark seismic “artefacts,” representing false features, and seismic washout effects, which are likely the result of the seismic pulse reflecting off of the concrete bulkheads of the canal walls or buried pipeline creating a hard seismic return signal.

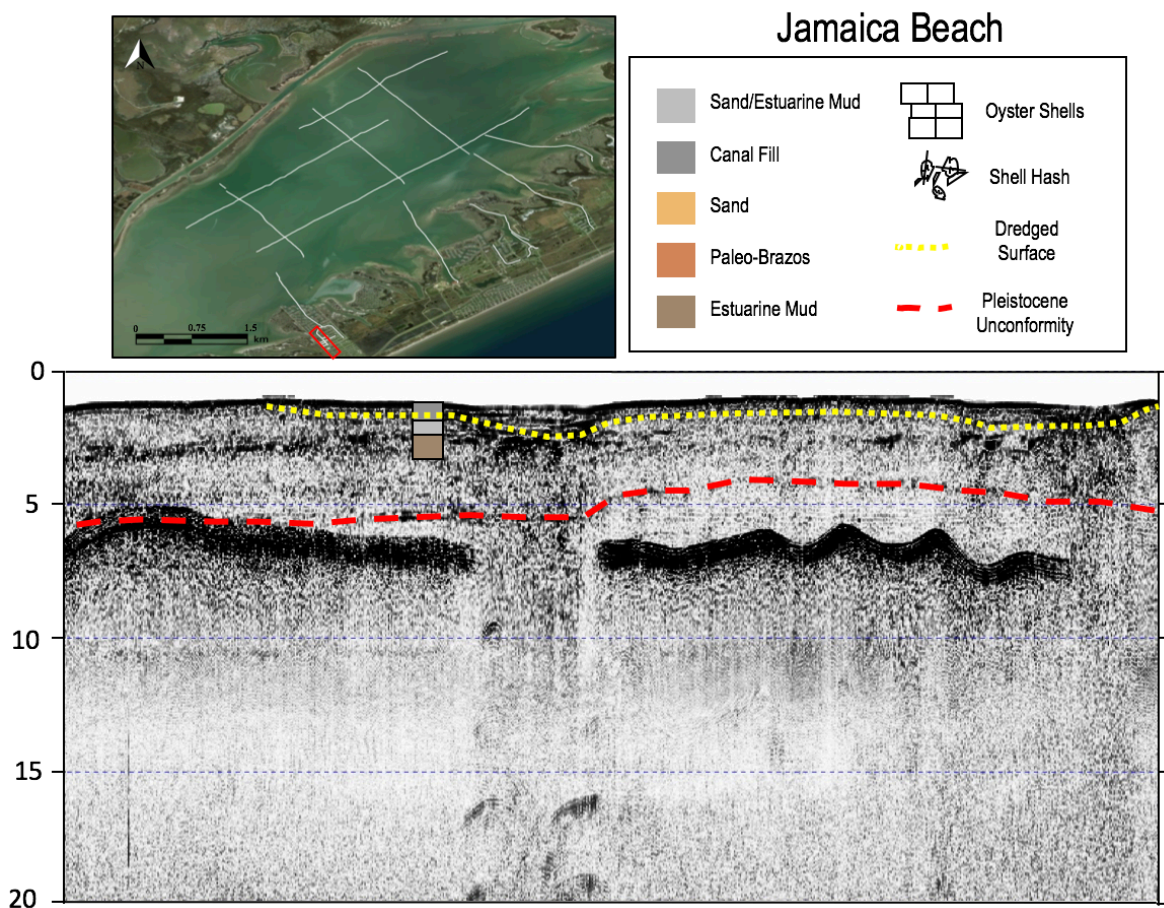


Figure 9. Core/SBP of Jamaica Beach. Sub-bottom Profile (SBP) in the canal of Jamaica Beach. A core description over the seismic image with its lithology depicted. The interpreted surfaces include the Dredged Surface in yellow and the Pleistocene Unconformity in red.

5.2 Interpolated Pleistocene Unconformity – 3D Surface

Correlations were found between the seismic data and sediment cores by observing the erosional features and stratigraphic transitions within the seismic images and the described lithology. Earlier findings from Lavery (2014) identified and named incised-valleys on the most western side of WGB by correlating the seismic data with sediment cores collected in the area. These findings were used as an initial guide for defining the seismic reflector that represents the Pleistocene Unconformity. Once the PU reflector was identified and traced within all the newly collected and reprocessed seismic lines, surfaces were created to visually display the antecedent topography beneath WGB.

Using the traces, x, y, z data were extracted from SonarWiz to generate a three-dimensional surface of the PU using the kriging interpolation tool in Arcmap (**Fig. 10**). The surface was generated with a 20-m cell size. The survey was separated into two mapped sections by a small terrace below present day Carancahua Reef, which is an oyster reef that extends north-south, bisecting the entire bay. Due to the shallow water depths over Carancahua Reef, we were unable to collect seismic data across the reef. Since the reef is a middle point between the two surveys, the area was used as a divider between the surface maps. Each section is identified as the eastern West Galveston Bay (EWGB), central West Galveston Bay (CWGB), and western West Galveston Bay (WWGB) (**Fig. 11**).

The PU surface in EWGB contains the Highland Bayou Incised-Valley (HBIV), which extends from the north shore of EWGB, where it meanders along the a axis, encompassing a majority of the eastern half of EWGB. HBIV ranges in width from 0.65 to 1.3 km wide, when measured normal to the axis of the channel. HBIV is named from the modern-day Highland

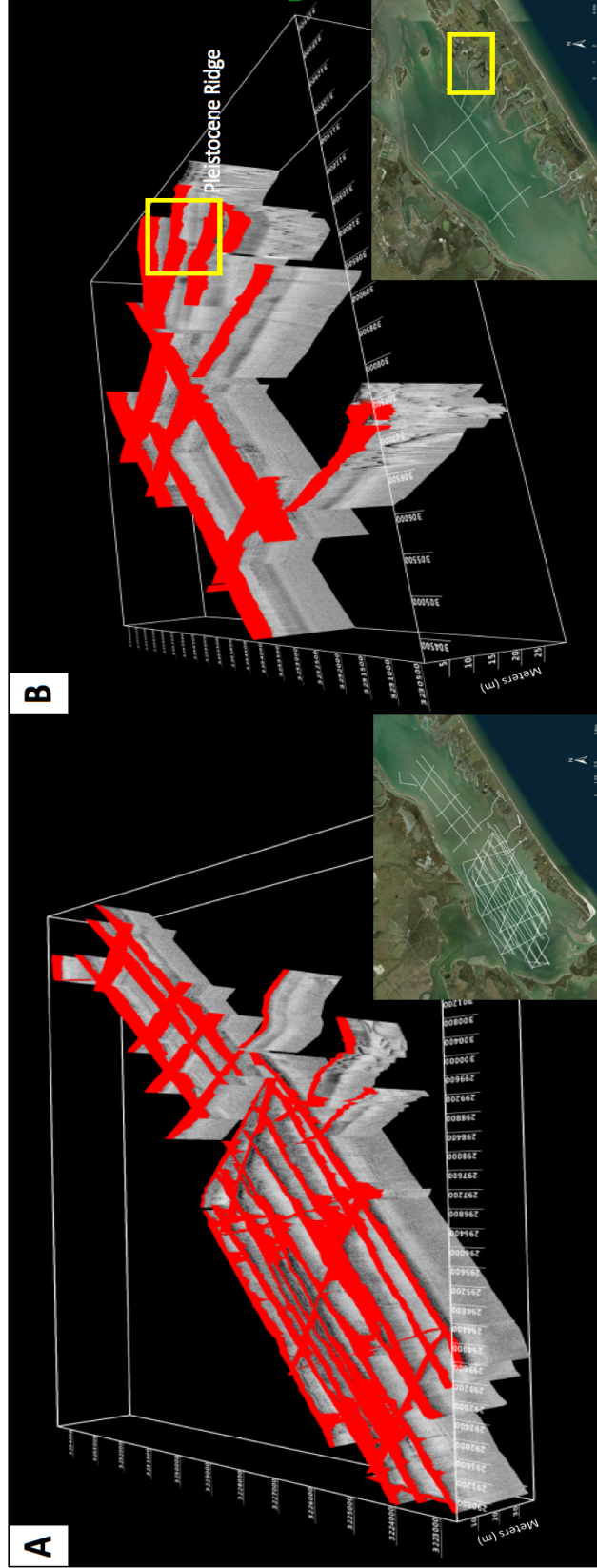


Figure 10. Fence Diagram of Pleistocene Unconformity. A. The Holocene sediment thickness of the western side of Carancahua Reef. B. Holocene sediment thickness eastern side of Carancahua Reef. The base of the thickness is the incision depth of the incised-valleys. The yellow box marks the Pleistocene ridge believed to have been the area of initial barrier formation of Galveston Island.

Bayou located the north part of the interpreted channel and the WBG shoreline, where its floodplain of the marsh/embayment is about 1.8 km wide. The western edge of HBIV is demarcated by a small terrace, which resides below modern-day Carancahua Reef (**Fig. 11a**). A small incised system is revealed within the CWGB with a similar orientation to the incised-valley found in the EWGB (**Fig. 11b**). The small valley is interpreted as the Eastern Halls Bayou Incised-Valley (EHBIV) and was a seaward extension of modern Halls Bayou. The valley connects to the larger Carancahua Incised-Valley (CIV) at the northern side Galveston Island. CIV was interpreted as a larger channel named for the Carancahua Lake on the north side of WGB. The CIV channel ranges in width between 0.8 and 1.4 km and the marsh, north of the WGB shoreline, is 1.9 km wide. This incised-valley is interpreted as an extension of an abandoned channel edged by a smaller terrace to the east, which extends below the modern-day Carancahua Reef. The interpreted Pleistocene surface within the canals of Galveston Island has an average depth of 5 m and can be identified up to 1.2 km into the interior of the island. The average PU surface depth, mapped up to 5 km into the interior of Galveston Island via canals, is shallower than the average surface depth across the 10.5 km of open water across WGB. A Pleistocene ridge was interpreted at -6 m below MSL within an unnamed canal between Sweetwater Lake and Sydnor Bayou (**Fig. 10b**). This canal is not labelled on the local NOAA charts and was named Tim Bayou for this study. The location of Tim Bayou is near the oldest section of Galveston Island. The presence of a ridge correlates with previous studies of the formation and geomorphology of Galveston Island (Bernard et al, 1970; Morton and McGowen, 1980).

5.3 Geometry of Incised-Valleys

To accurately define the base of the incised-valleys, an erosional surface was interpreted as a prominent dark reflector signifying a change in acoustic impedance within the seismic data throughout WGB. This dark reflector truncates uniform, sub-parallel Pleistocene reflectors. Evidence of abrupt truncation along the high amplitude

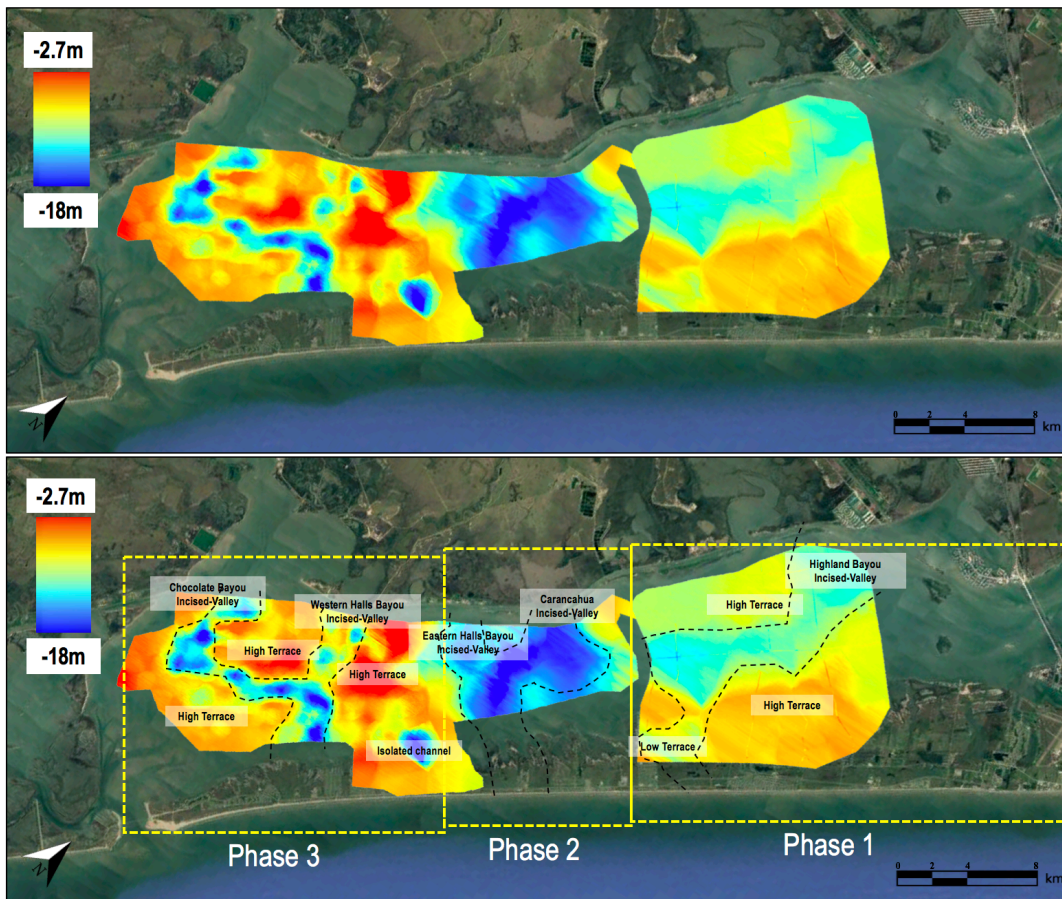


Figure 11. Pleistocene Unconformity Distribution of West Galveston Bay.
A. Uninterpreted surface of the PU. B. Interpreted PU surface. The yellow boxes represent the sections of formation of Galveston Island.

reflectors are a clear indicator of the presence of an incised-valley. The Pleistocene/Holocene boundary throughout the study area has similar characteristics easily identifying the surface, but each channel has differences in their size and shape.

In EWGB, an incised-valley was mapped and named the Highland Bayou Incised-Valley (HBIV). It lies below the Holocene strata and extends seaward beneath present-day Jamaica Beach and Carancahua Cove (**Fig. 11**). HBIV is a wide, box-shaped channel with an average depth of -7 m and a maximum depth of -12 m. The average channel width in the valley axis in the normal direction is 1.7 km, making it the widest in the WGB system (**Fig. 12a**). This channel has an irregular cross-sectional profile when compared to the others within WGB. HBIV is bounded by symmetric gentle-sloping walls to the maximum depth of incision. Fluvial and estuarine strata was deposited above the Pleistocene unconformity during the Holocene and the channel was previously unidentified.

Eastern Halls Bayou Incised-Valley (EHBIV) and Carancahua Incised-Valley (CIV) were identified beneath the central part of the WGB estuary. Both are named after their distributaries on the mainland, Halls Bayou and Carancahua Lake (**Fig. 12b**). The EHBIV connects to CIV near the north side of Galveston Island between present-day Maggies and Bird Island Coves and extends in the seaward direction, presumably under the modern Galveston Island. The EHBIV has a box-shaped geometry with sets of downstepping terraces along its boundary at -7 m and -9 m below MSL (**Fig. 12b**). The average width of the valley. Measured in the direction perpendicular to the axis of the valley, is 0.65 km. Based off of interpretations from the seismic lines, the lower 6-8 m of the Holocene channel fill consists of laminated strata, but the upper 4m contains dipping beds suggesting a prograding bayhead delta deposit. CIV in CWGB is the deepest channel in WGB, with a maximum depth of -18 m. The valley has an average depth of 8 m, with a wide box-shaped geometry and an average width of 1.2 km.

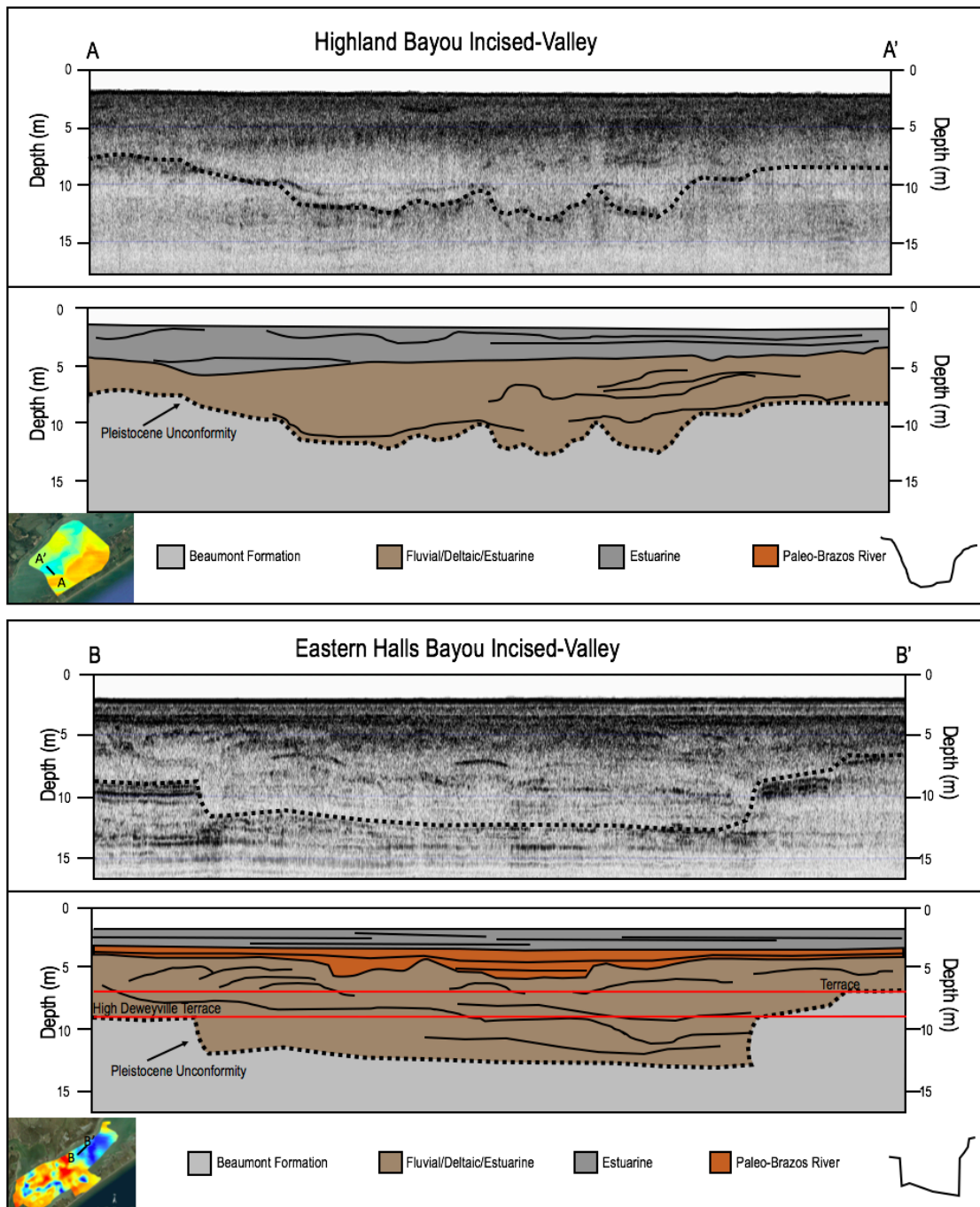


Figure 12. Cross Section of the Highland Bayou Incised-Valley and the Eastern Halls Bayou Incised-Valley. A. Cross-section of the Highland Bayou Incised-Valley. B. Cross-section of the Eastern Halls Bayou Incised-Valley with the seismic image and facies description of valley fill. The red lines mark the terraces within the valleys. Cross-section profile of the channel is in black.

In the westernmost portion of WGB, Lavery (2014) mapped out the Chocolate Bayou Incised-Valley (CBIV) across the western half of WGB. The CBIV has an average depth of 6 m, with its maximum depth of -17.74 m below MSL. It is a wide, deep channel with a combination of V and box-shaped geometries and an average width of 1.07 km (**Fig. 13b**). Downstepping terraces were observed on the eastern side of the channel at -5, -6.5, and -8 m below MSL, suggesting that CBIV is a compound rather than a simple valley. The CBIV is filled with fluvial and estuarine strata. Even though the Chocolate and Halls Bayou Incised-Valleys are in the same study area and merge into a single valley, they have very different depths and characteristics. The Western Halls Bayou Incised-Valley (WHBIV) has an average depth of -3 m. It is described as a narrow, shallow channel with a box-shaped geometry and has an average width of 0.5 km (**Fig. 13a**). The lack of terraces around this channel suggests that it is a simple incised-valley. The depositional features contained within the Holocene strata, including uniform laminations, hint to a high rate of deposition. The valleys merge into a single valley and the merged valley extends seaward beneath Galveston Island. Large storm surge channels and overwash fans exist above where the valley extends under the island (**Fig. 14**).

5.4 Interpreted Paleo-Brazos River Surface

The Paleo-Brazos River (PBR) deposits were observed within the CHIRP seismic data as a dark, uniform reflector and was thoroughly mapped within WWGB (**Fig. 15**). The deposits were found in cores as a red, oxidized clay in sediment cores, specifically in the Terramar Beach canal and isolated Indian Beach Bayou channel on the western end of Galveston Island (**Fig. 16**). The deposits were easily recognized as a red clay within the core, above which it transitions into gray-black estuarine mud. The top of the PBR deposits in the Terramar Beach core is at 3.2 m

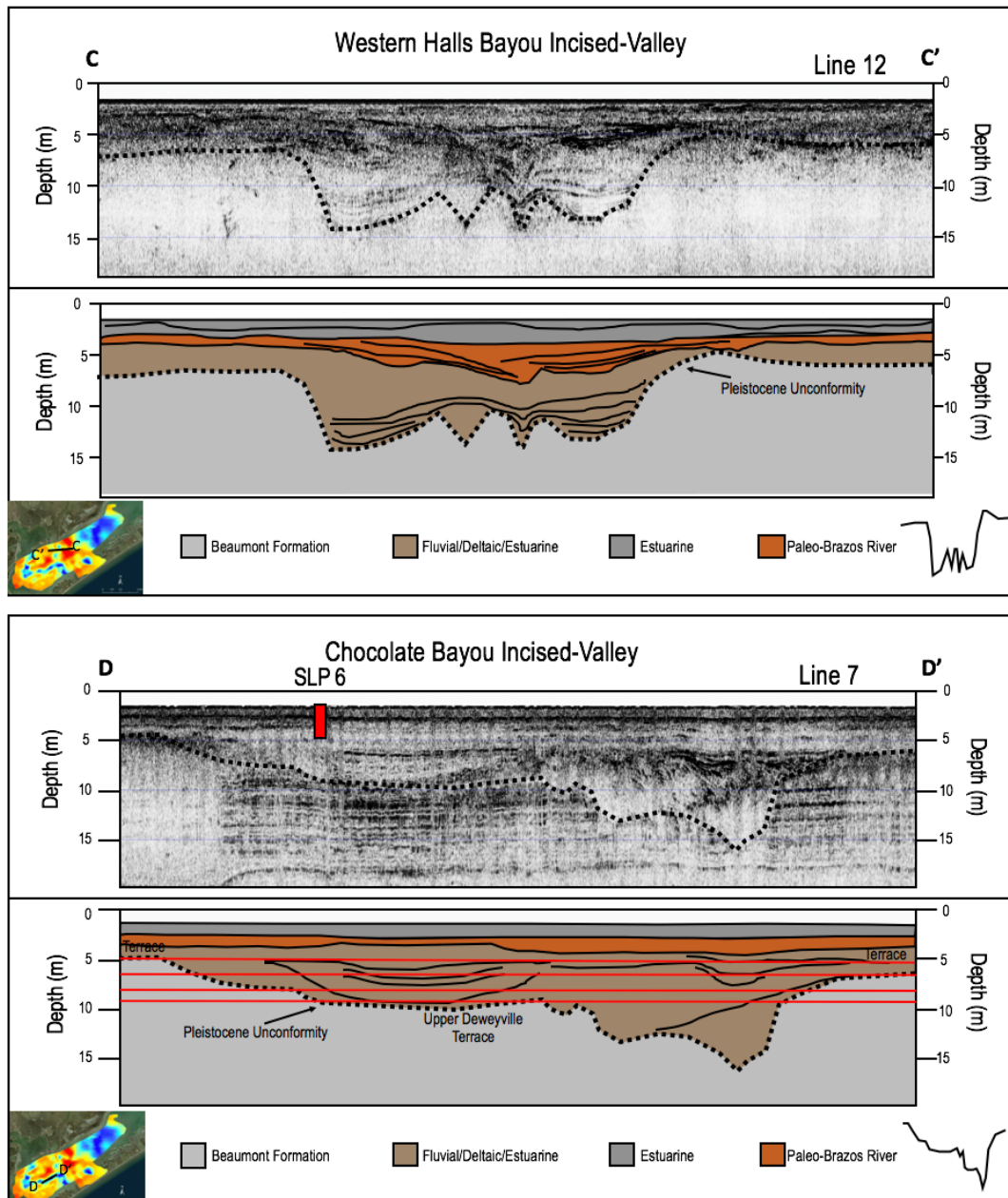


Figure 13. Cross Section of the Chocolate Bayou and Western Halls Bayou Incised-Valley. A. Cross-section of the Western Halls Bayou Incised-Valley. B. Cross-section of the Chocolate Bayou Incised-Valley with the seismic image and facies description of valley fill. The red lines mark the terraces within the valleys. The SLP 6 core in red shows the Estuarine and Paleo-Brazos sediment, from Laverty (2014). Cross-section profile of the channel is in black.

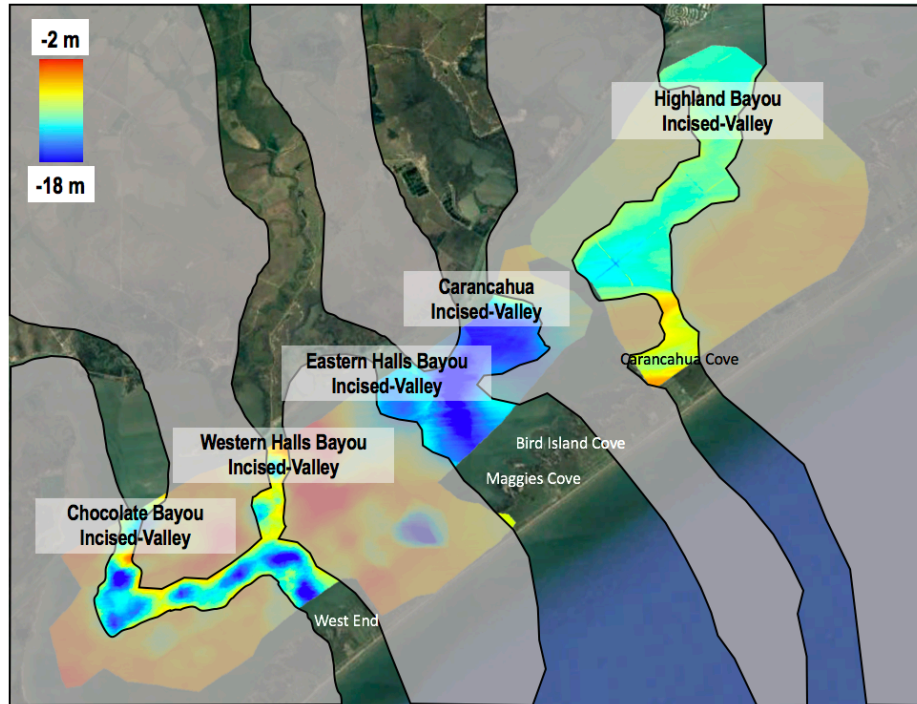


Figure 14. Interpreted Path of West Galveston Bay Incised-Valleys.
The proposed path of the incised-valleys found within West Galveston Bay.

below MSL and is 1.15 m thick, with the base of the core at 4.35 m (**Fig. 16**). In the Indian Beach Bayou core, which was collected 7.6 km northeast of the Terramar Beach core site, the top of the PBR layer is 4.2 m below MSL and is 1.6 m thick, with the sediment transition to estuarine mud at 5.8 m (**Fig. 16**). Evidence of the PBR was not present within the seismic lines or sediment cores collected in EWGB, suggesting that it was not deposited east of Carancahua Reef. A twig collected at the top of the Indian Beach Bayou PBR layer was dated at 5033-5189 yBP. The Indian Bayou sediment core was correlated with SLP 27 core, collected from (Lavery, 2014) with similar elevation. A sediment core collected by Lavery (2014) contained a PBR layer at 3.1 m below MSL. A sample collected from the top of the PBR layer was dated at 4390 yBP. Both cores contain PBR deposits with similar thicknesses, but the top of the sediment layer has a 1,000-year difference, suggesting erosion at the surface of the Indian Bayou PBR deposit.

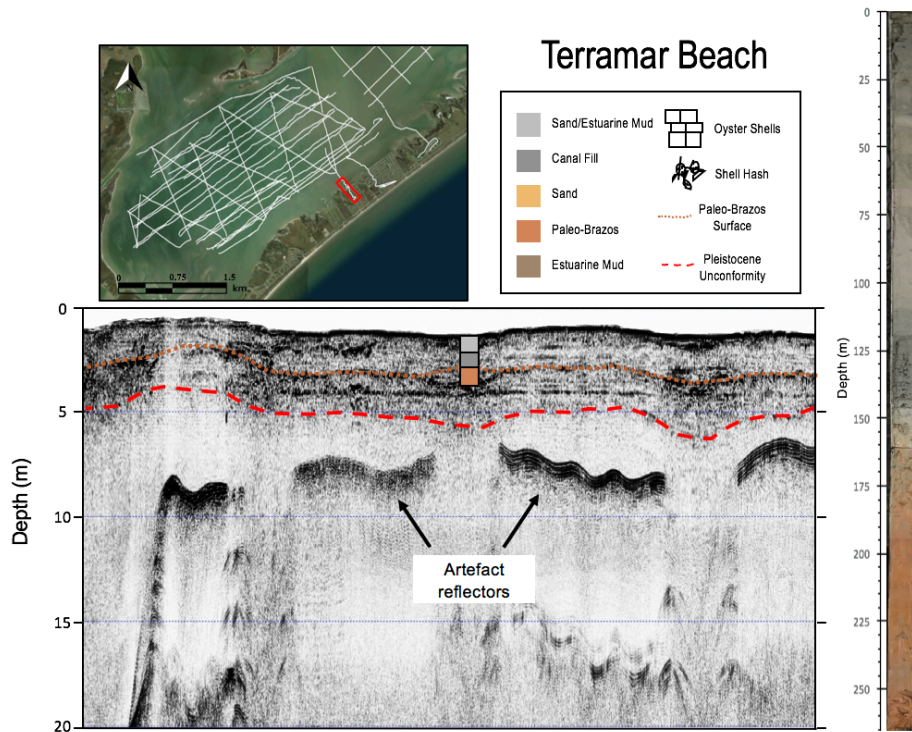


Figure 15. A. Core/SBP of Terramar Beach. The core description of Terramar Beach sediment core over the seismic image. B. Core photograph of Terramar Beach core.

5.5 Geomorphology

Google Earth aerial photo mosaics from 1954 were observed to document the geomorphic features and change in width of Galveston Island (**Fig. 7**). The early images are from the period prior to significant development of the west end of Galveston Island and were used to observe the natural state of the barrier island prior to development which altered the landscape. Along the oldest section of the island, near Sweetwater Lake and Lake Madeline, the island is 3.77 km wide, this is also the islands widest point. Carancahua Cove and Jamaica Beach is 16.93 km SW of Lake Madeline and where HBIV is interpreted to extend seaward beneath Galveston Island. This area contains two coves and seven storm surge channels. The width of the island at Jamaica Beach is 1.69 km. The section of Galveston Island that sits atop the CIV/EHBIV is

located at Maggies and Bird Island Cove and has a width of 1.5 km. EHBIV and CBIV is interpreted beneath an unnamed overwash site on the west end of Galveston Island. The location of the most eastern buried, paleo-channel crossing beneath Galveston Island decreases the overall width of the island from 1.5 km to 1.33 km. The number of features also decreases from one washover site, one storm surge channel, and two embayments to no significant features or indicators of island breaching, storm surge channel formation, or sediment scouring.

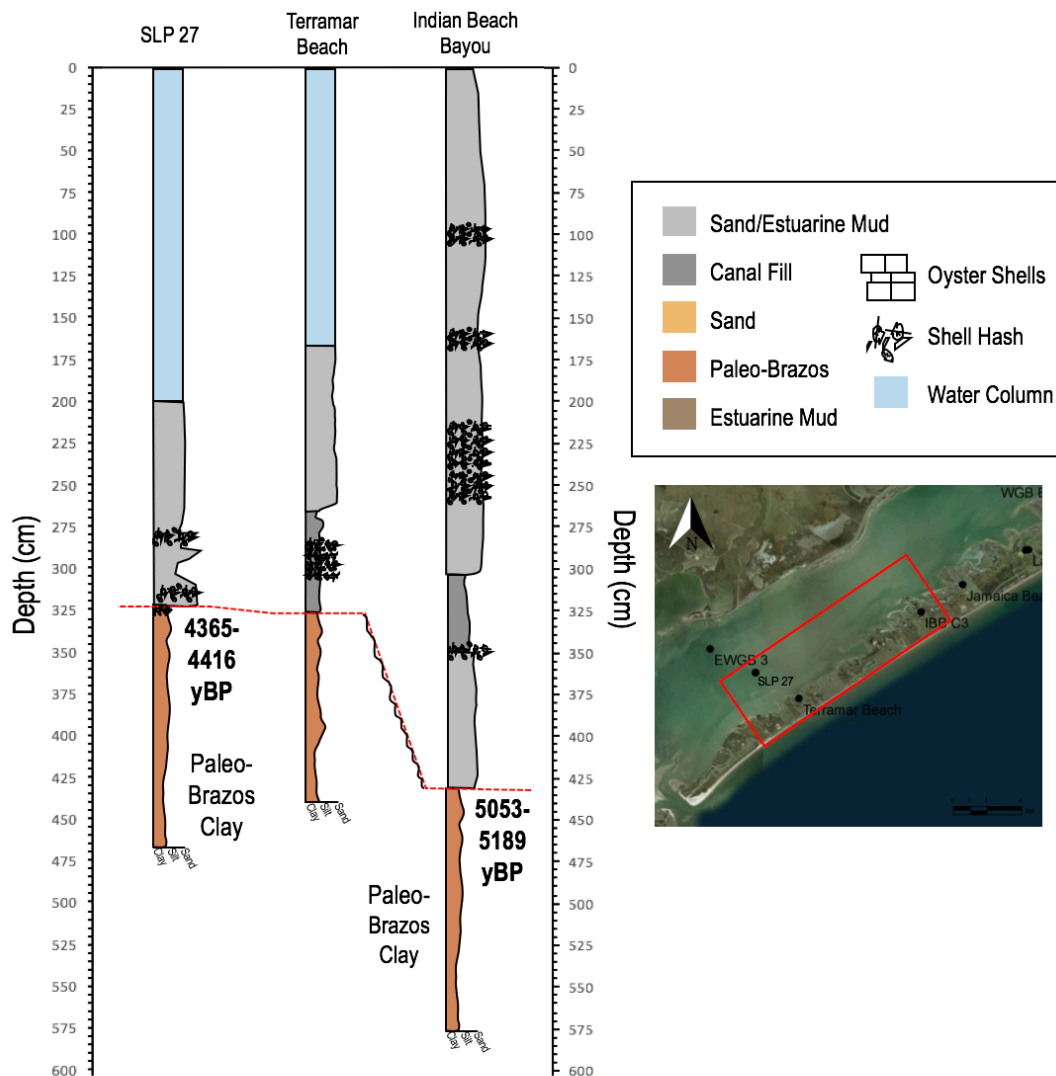


Figure 16. Core Descriptions of Terramar Beach, Indian Beach Bayou, and SLP 27. The red line marks the Paleo-Brazos to estuarine mud transition. Reference map shows the location of Terramar Beach within Galveston Island.

5.6 Storm Surge Channels

The storm surge channels found along the bay-side of Galveston Island are perpendicular to the shoreface and beach ridges. When formed and active, the storm surge channels cut through the island, including cutting through beach ridges during storm surge overwash and provides a conduit for storm surge ebb, further incising the channel. The seismic data and aerial images of the canals within Galveston Island showed a relation between the location of incised-valleys and the size of surge channels above all the incised-valleys identified in this study. Three sections of incised-valley systems, HBIV, CIV/EHBIV, and CBIV, extend seaward beneath Galveston Island (**Fig. 11**). High resolution seismic data from within Jamaica Beach and Echert Bayou

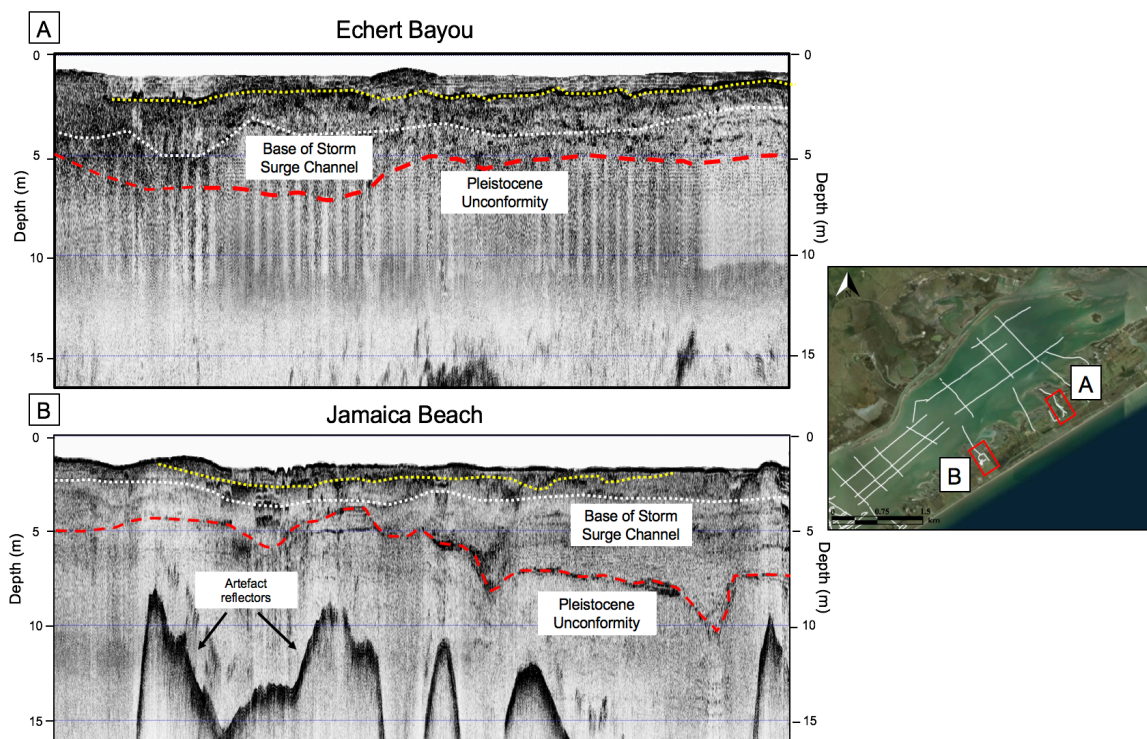


Figure 17. SBP of Echert Bayou and Jamaica Beach. A. Seismic image of the Echert Bayou storm surge channel showing the base of the channel and the Pleistocene Unconformity. B Seismic image of the Jamaica Beach storm surge channel showing the base of the channel and the Pleistocene Unconformity. Reference map shows the location of the SBP lines within Echert Bayou and Jamaica Beach. Yellow is the Dredged surface. White is base of Storm Surge Channel. Red is Pleistocene Unconformity.

canal (**Fig. 17a and Fig. 17b**) reveals a small, dark, box-shaped reflector above the PU surface with high amplitude surrounded by Holocene sediment. The reflectors show stratal laminations representing the repeated deposition of sand filled storm surges interbedded with darker estuarine mud. Jamaica Beach is one of the storm surge channels with an incised-valley (maximum depth of -10 m) beneath the storm surge channel (**Fig. 17b**).

Along the widest section of Galveston Island, around Sweetwater Lake, there are 22 sets of nearly continuous beach ridges and swales, with three breach sites (**Fig. 7**). Around Echert Bayou, 6 km southwest of Sweetwater Lake, there are 10 sets of beach ridges and swales with no breach sites. There are three storm surge channels with widths greater than 50 m between Sweetwater Lake and Echert Bayou. Along Jamaica Beach, 12 km to the southwest of Sweetwater Lake, there are only 2 sets of beach ridges and swales with no breach sites. Both sets are close to the beach, representing the island's accretion seaward. Eight large storm surge channels are located between Echert Bayou and Jamaica Beach (**Fig. 7**), with the channels extending furthest into the island. Maggies Cove, 17.1 km SW of Sweetwater Lake, has no beach ridges or swales. There are 10 storm surge channels between Jamaica Beach and Maggies Cove, two of them reach 1 km from the shoreface. On the West end of the island at an overwash site 22.7 km west of Sweetwater Lake, there are no signs of beach ridges and swales. Five major storm surge channels lie between Maggies Cove and the overwash site. The last few kms between the overwash site and the west end of the island has one major storm surge channel, with the island width reducing the ability for overwash or breaching.

5.7 Geotechnical Properties

The WGB3 and PIB-2 cores were collected to obtain a fresh Pleistocene sediment sample. The both sites were used due to the high elevation of the PU at <2 m from the subsurface to ensure Pleistocene sample collection (**Fig. 18**). Shear strength and compressive strength was determined from the cores along 10 cm intervals, including both above and below the PU. As discussed above, shear strength is an indication of resistance to erosion. Pleistocene paleosol is more cohesive than soft Holocene mud. The shear strength and compressive strength of sediment also typically increases with depth (Wallace et al, 2009). The typical shear strength of the Pleistocene in the upper Texas coast is greater than 1 kg cm^{-2} , which is a high shear strength compared to the Holocene shear strength of $0.05\text{-}0.10 \text{ kg cm}^{-2}$ (Rodriguez et al, 2001). The shear strength of both cores was measured using a Pocket Torvane Shear tester. The WGB3 Holocene sediment had shear strength values from $0.02\text{-}0.04 \text{ kg cm}^{-2}$. The Pleistocene sediment had a measured shear strength from 0.7 to 1 kg cm^{-2} . The basal 10 cm of the core contained the sediment from both sequences interbedded, causing a lower shear strength for the Pleistocene sediment. For PIB-2, the Holocene sediment had a shear strength from $0.04\text{-}0.10 \text{ kg cm}^{-2}$. The Pleistocene samples were $0.5\text{-}0.7 \text{ kg cm}^{-2}$, less than the typical value, however, the measured shear strength of the Holocene sediment is only 8-14% of the measures Pleistocene sediment shear strengths. Compressive Strength was measured using a pocket penetrometer and is a quantitative measurement of sediment compressibility and its resistance to compaction. The WGB3 Holocene sediment samples had measured compressive strength of $0.06\text{-}0.08 \text{ kg cm}^{-2}$. The Pleistocene sediment was a magnitude higher with values $0.13\text{-}0.22 \text{ kg cm}^{-2}$. The compressive strength was not measured for the PIB-2 core because the samples were used for another study before measurements were taken. Both methods are simple, lightweight

instruments to obtain a quick classification of cohesive sediment and can be subjected to measurement errors. A solution was to make multiple measurements and calculate an average.

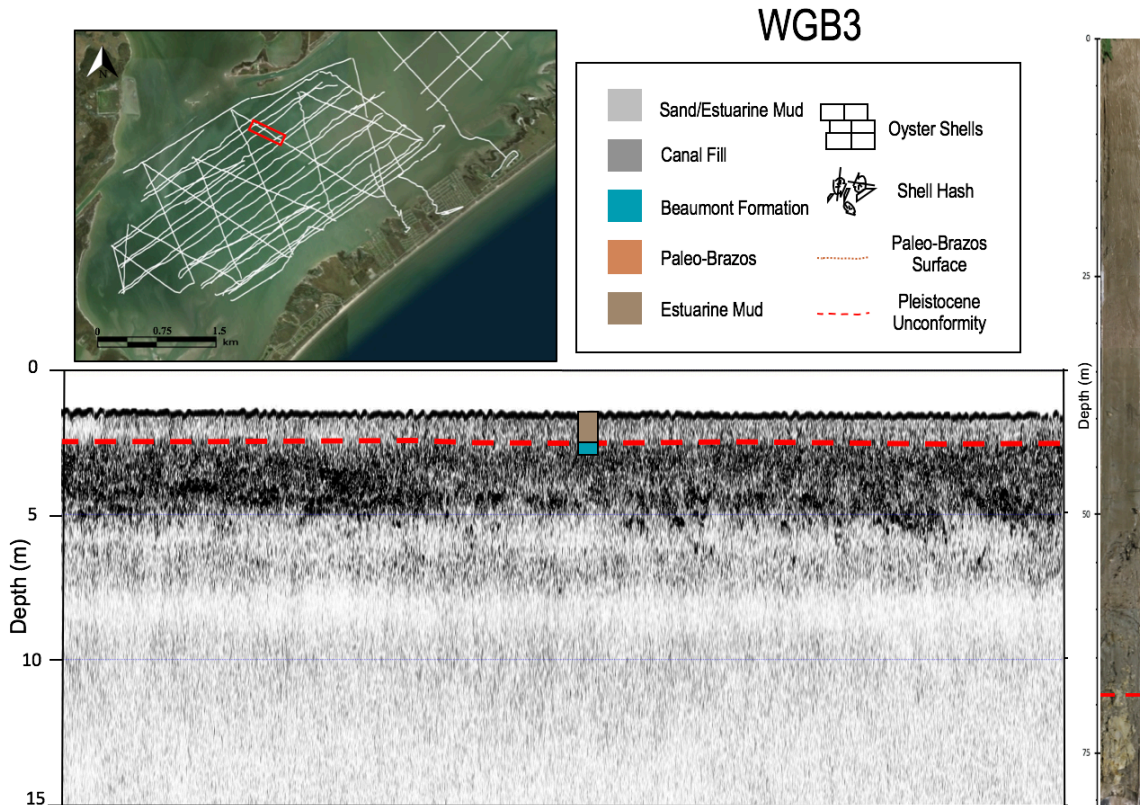


Figure 18. SBP and Core photo of WGB3. The core lithology is depicted over the seismic image. The interpreted Pleistocene Unconformity is outlined in red.

5.8 Subsurface Facies

The stratigraphy preserved within the incised-valleys contain a record of the changes in the depositional environment of WGB during the Holocene. The abandoned distributaries contain strata from fluvial to Paleo-Brazos River deltaic and estuarine mud. The objective was to identify the PU and the distribution of the PBR deposits. Four facies were identified, which are: 1) Modern Estuarine Canal Fill, 2) WGB Estuarine, and 3) Paleo-Brazos Delta Mud, and 4) Beaumont Formation

Facies Descriptions:

1) Modern Estuarine Canal Fill: Gray to black sandy mud, high water content mud, with little to no sand and few if any shells, some evidence of bioturbation (anoxic sediment); in the seismic data, it is characterized as acoustically transparent, with its base marked by a dark, irregular reflector.

2) WGB Estuarine: brown to grey silty to sandy mud and muddy sand, very little to no sand intervals, sections of shell hash interbedded in mud, low shear strength. The facies contain modern estuarine mud and basal sandy and muddy sand from bayhead delta deposits (Lavery, 2014); in the seismic data, it is characterized as having a range of low to moderate amplitude reflectors which can be discontinuous and chaotic, or transparent.

3) Paleo-Brazos Delta: highly oxidized red to orange-brown clay with interspersed shell fragments, moderate water content; in the seismic data, it is characterized as a thin layer with parallel, high amplitude reflector

4) Beaumont Formation: yellowish to green, hard, consolidated clay or paleosol, low water content, high shear strength; in the seismic data, its surface is characterized as having a dark, high amplitude reflector with sub-parallel, truncated horizons below.

An idealized stratigraphic column within the incised-valleys of the WGB system contains the Beaumont Formation at its base, which consists of very hard, consolidated, paleosol clay with a higher shear strength. The Holocene sequence begins with the paleo-WGB Estuarine deposits, which contains mud with interspersed shell hash and oyster reef deposits, the facies contains an older sequence of basal sand and muddy sand from bayhead deposits (Lavery, 2014). It should be noted that in this study, the bayhead delta deposits are not being differentiated from the estuarine deposits. This is because the bayhead delta deposits were not

sampled in the study cores. It wasn't part of the main focus, which is to map the major stratigraphic intervals primarily based off seismic interpretations. Where the deposits were found, the Paleo-Brazos Delta consists of a relatively uniform reddish-brown clay with minor shell fragments throughout the layer. The PBR deposits separate the WGB Estuarine between a modern estuarine mud and older basal muddy sand in the CWGB and WWGB, but not the EWGB, where the WGB Estuarine facies is one sequence. The Estuarine fill lies above the Paleo-Brazos, contains sparse oyster and bivalve shells and a low sand content and lower shear strength and higher water content than the Paleo WGB Estuarine deposit. Within the dredged canals, there exists the Modern Estuarine Canal Fill (**Fig. 19**). Only two cores collected in this study, WGB3 and PIB-2 contain both the Paleo WGB Estuarine and the Beaumont Formation deposits (**Fig. 18**). All the cores collected in the canals contained Modern Estuarine Canal Fill, a high-water content (soupy) mud layer, above the lower water content WGB Estuarine deposits. The transition from high-water content mud to semi-consolidated mud represents the dredged surface within the canals and was observed in the seismic data as a dark reflector above the lighter undisturbed sediment. No Paleo-Brazos Delta deposits were found within the cores collected in the canals east of Carancahua Reef or in EWGB. The shallow depth of the Pleistocene surface suggests that this site may have been too topographically high to accumulate recent sediment deposition and to preserve Paleo-Brazos sediment in this location if it had even been dispersed this far east.

Sediment cores collected from Lake Madeline, Spanish Grant, and Echert Bayou (**Fig. 20**) each contain the Modern Estuarine Canal Fill as a small interval of grey sandy mud in the upper 50 cm, which represents the recent deposited sediment in the canals. Below this layer is a series of thicker beds (25-75 cm) of well sorted, fine to medium fine sand interspersed with

discrete intervals of shell gravel (shell hash). These sand beds were deposited from the oldest parts of barrier island formation. The abundance of sand in these cores located in the oldest section of the island capture the 1st phase of island growth by showing an abundance of coarse sediment in the upper 3 m of the island. The sediment cores collected within the canals of Galveston Island (Fig. 20) show a steady transition of the island's growth phases from the East

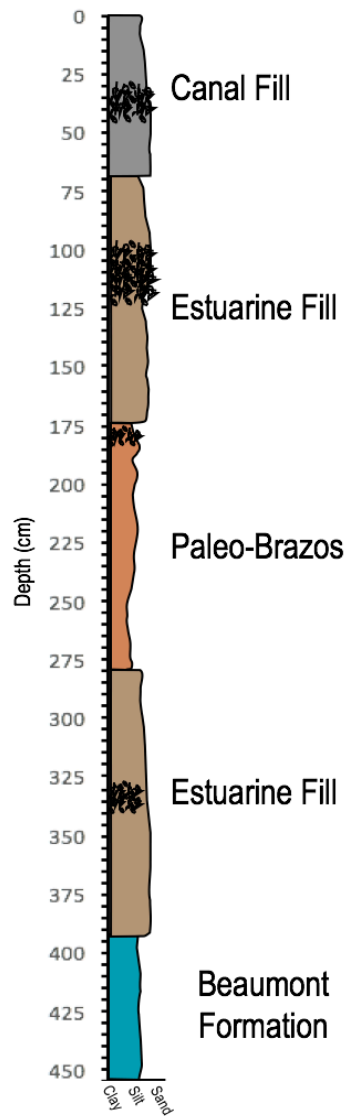


Figure 19. The Ideal Stratigraphic Column of West Galveston Bay.

to West. Cores from Jamaica Beach and Lake Como have no well sorted sand intervals, instead there are interspersed large sandy and estuarine mud layers intermitted with shell gravel. The lack of sand in these cores show a transition from barrier island to estuary environments. This transition represents the island's accretion seaward and the 2nd phase of island growth. Cores from Indian Beach Bayou and Terramar Beach contain an interval of the Paleo-Brazos Delta as an oxidized red clay, which is PBR sediment 4.25 m and 3.6 m below MSL, respectively. There are no well sorted sand intervals in these cores, just sections of dark, muddy sand and sandy mud (Modern Estuarine Canal Fill and WGB Estuarine). The cores did not reach the estuarine mud layer below the fluvial deposits. Indian Beach Bayou is a healed, isolated storm surge channel and shows the accumulation of island sediment as muddy sand with frequent shell hash layers most likely from local overwash/flooding events.

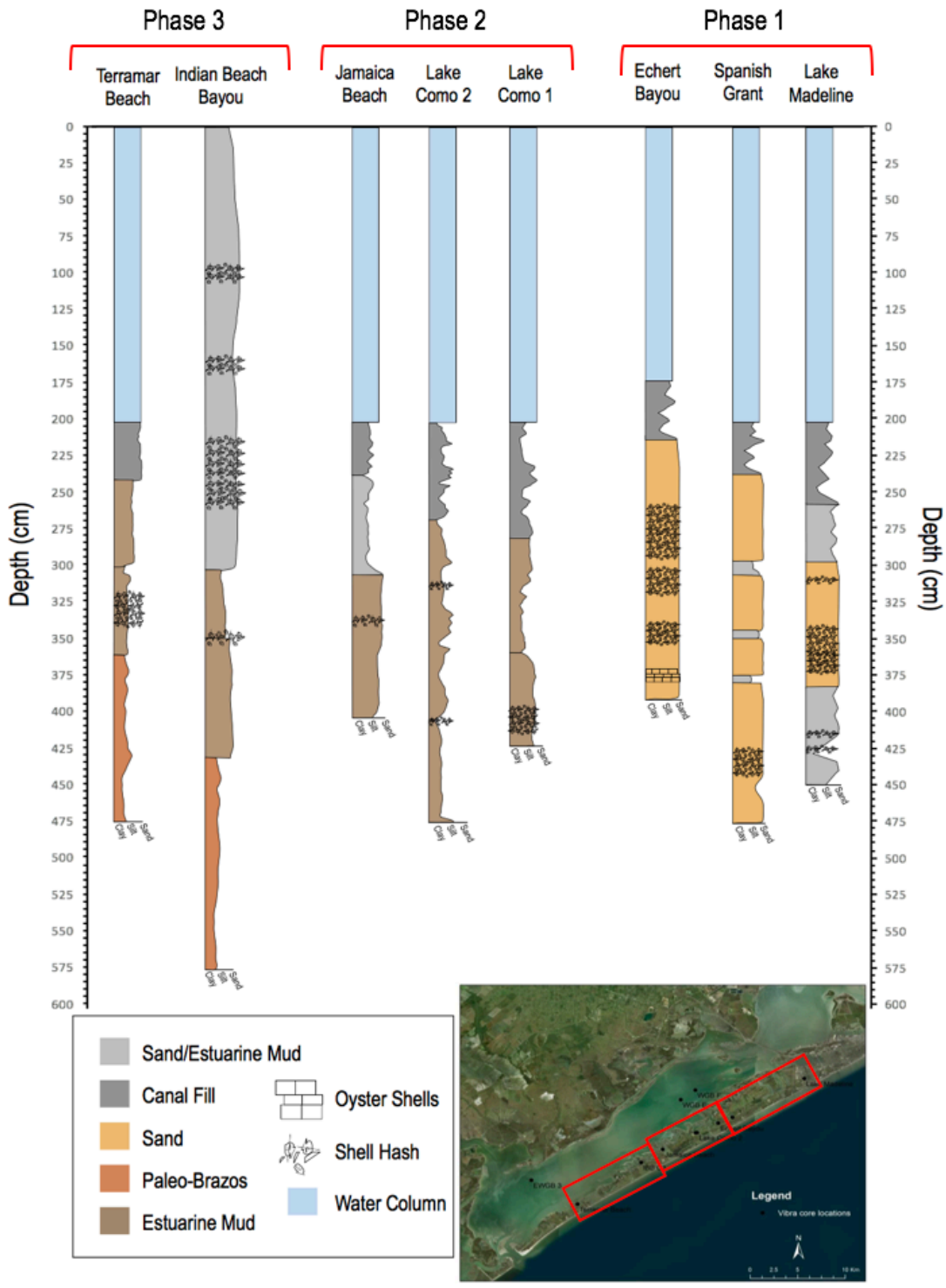


Figure 20. Core Descriptions of Galveston Island Cores. Core descriptions of the cores collected within Galveston Island and canals. The red box highlights the section of cores.

6. DISCUSSION

The hypothesis for this study is stated as: Topographic variations of the antecedent Pleistocene surface of the WGB system was a major control during the formation and evolution of Galveston Island. The discussion will illustrate how this study determined how the topography of the Pleistocene surface influenced the geomorphic features and evolution of Galveston Island and WGB.

6.1 Formation and Type of Incised-Valleys

6.1.1 Eastern West Galveston Bay

This study answered the question: Incised-valleys were found on the most western sections of WGB, is there a network of incised-valleys on the eastern half of WGB? This was determined by mapping the network of incised-valleys beneath WGB. The geometry of an incised-valley can be used to classify the valley type, correlate the maximum depth of incision to a local sea level curve, and determine the timing of channel flooding by the rising sea level. Piedmont incised-valleys along the northwestern Gulf of Mexico tend to be deep compound incised-valleys and are associated with larger river systems (Anderson et al, 2016) as well as contain terraces with an asymmetric cross-section (Nordfjord et al, 2005). Coastal-plain incised-valleys are associated with much smaller rivers and drainage basins and can be either simple or compound. The simple coastal-plain incised-valleys tend to be V-shaped and are typically symmetrical or have a wide base (Nordfjord et al, 2005).

In EWGB, HBIV extends seaward below present-day Jamaica Beach and Carancahua Cove. HBIV is interpreted as a wide, box-shaped channel with a maximum depth of -12 m and lacks terraces, making it a simple coastal-plain incised-valley (**Fig. 12a**). It should be noted that

the seismic line showing the cross-section of HBIV was collected at an oblique angle to the channel, making it appear much wider than it actually is. Its namesake, Highland Bayou is a watershed on the northeast side of WGB, which continues to deliver sand and mud into the bay. The modern marsh which located at the mouth of Highland Bayou, is over 4 km wide, suggesting a comparably large system formed the incised-valley that the marsh currently occupies. The HBIV geometry has the shallowest base level of the incised-valleys within WGB. It is characterized as a shallow incised-valley with an irregular cross-sectional profile when compared to the other incised-valleys within the WGB system. It is bounded by a gentle slope to the maximum depth of incision (**Fig. 12a**). The seismic interpretations show the maximum depth of incision at -12 m. According to the Milliken Sea Level Curve (Milliken et al, 2008), the sea level at -12 m occurred around 7,900 yBP, making the initial incision of the channel to occur pre-8,000 yBP, when the sea level was below -12 m. The seismic lines that show HBIV were collected from within the dredged canals at Jamaica Beach (**Fig. 10**). The base of the incised-valley is -10 m below MSL and coincides with the deepest depth of the PU surface beneath Galveston Island, when compared to other Galveston Island canal seismic lines. Within the vibracores, layers of oyster shells were found within the sediment cores and correlate to events observed in the seismic data in EWGB, indicating the presence of buried oyster reefs within the incised-valley sediment fill. The oyster reefs were -5 m below MSL and formed around 5,600-5,800 yBP, after a flooding event transitioned WGB from a bayhead delta to an estuary.

6.1.2 Central West Galveston Bay

The EHBIV and CIV sit below the present-day WGB estuary and merge into a single valley near the northern shore of Galveston Island, between present-day Maggies and Bird Island

Coves (**Fig. 11**). The EHBIV is interpreted as a small, box-shaped incised-valley with sets of terraces at -7 m on eastern slope the and -9 m on both sides below MSL (**Fig. 12b**). However, the placement of the -9 m terrace correlates with the High Deweyville terraces located within the Trinity River Incised-Valley beneath Galveston Bay (Rodriguez et al, 2005). The -7 m terrace is not related to the Deweyville terrace as it is too shallow; this terrace was most likely a part of the Beaumont terraces, which was independently formed from the river floodplain. A -5 m terrace present along the EHBIV is most likely a Beaumont terrace, which was formed before the Deweyville terraces, but flooded more recently. The presence of these terraces makes the EHBIV a compound incised-valley. The base of the EHBIV is -13 m below MSL, making the time of initial flooding around 8,200 yBP, marking the beginning of the deposition of estuarine deposits.

Carancahua Incised-Valley is a wide, box-shaped channel with a maximum depth at -18 m below MSL. The depth of the base level suggests the flooding surface occurring around 10,000 yBP. This is the deepest incised-valley in this study and has no terraces on the slope walls, indicating that it is a simple incised-valley. Since the CIV is the deepest channel in WGB, it was most likely the first channel to be flooded by the Holocene transgression. The CIV connects with EHBIV on the bay-side of Galveston Island and extends seaward beneath the island at Maggie's Cove and Bird Island Cove.

6.1.3 Western West Galveston Bay

The CBIV has characteristics of a wide, deep channel with a combination of V and box-shaped geometry with its maximum depth of -17.74 m below MSL. On the western side of the estuary, the channel contains sets of downstepping terraces (**Fig. 13b**), consistent with compound valley nomenclature. The terraces within the CBIV are located at -5 m and -7 m on the eastern

wall, -8 m on the western walls, and -9.5 m on both sides. Only the -9.5 m terraces correlates to the High Deweyville terrace found within the Trinity River Incised-Valley beneath Galveston Bay. The High Deweyville terrace was buried by Holocene sediment during and after the 7,700 yBP flooding event, which can suggest that CBIV was inundated at that time. The other terraces at -7 m and -8 m, do not correlate to specifically established Deweyville terraces found in the literature, and were inundated 7,100-7,300 yBP. The base level of the valley is at -17.74 m and was initially flooded by rising sea level around 9,900 yBP.

WHBIV is a shallow channel with a box-shaped cross-sectional profile with steep slope walls and lacking terraces (**Fig. 13a**). With an average 0.5 km width, WHBIV is a relatively narrow channel with a base level at a maximum of -15 m below MSL, whereas CBIV has an average width of 1.07 km and a base level of -17.74 m. Even though the CBIV and WHBIV are in the same study area and merge into a single channel, the two channels have significantly different depths and characteristics. Downstream of where the channels connect and extend seaward beneath an area of Galveston Island, large storm surge channels and overwash fans reach into the interior of Galveston Island.

In summary, CBIV and EHBV are compound incised-valleys indicating that these valleys were likely formed by a large fluvial system than their namesakes. As discussed in the next section, the paleo-Brazos River has shifted course many times and has flowed into WBG even during the Holocene. In fact, during Hurricane Harvey in 2017, the Brazos River breached its banks and flowed into Chocolate Bayou. Anderson et al (2016) shows a Stage 53 (~120 kya) Brazos Delta occupying the position currently occupied by WBG and it is likely these compound incised-valleys were originally formed during Stage 5e then the incised-valleys were re-occupied by their namesake rivers/bayous either during the late Pleistocene or early Holocene. This would

suggest these incised-valleys were originally formed as piedmont incised-valleys rather than coastal-plain incised-valleys. The extent of the Pleistocene terraces indicates that the outline of the piedmont Pleistocene incised-valley is much wider than the portion of the valley with Holocene fill. Based on the extent of the Pleistocene terraces, it is reasonable to assume that the piedmont incised-valley extended as far east as present day Carancahua Reef and may connect to the west with the modern Brazos Incised-Valley. This further suggests that the presence of terraces, i.e. compound valleys are indications of piedmont valleys rather than coastal-plain valleys at least in this portion of the northwestern Gulf of Mexico.

6.2 Paleo-Brazos River

Between 6,600-4,000 years ago, the Paleo-Brazos River Bayhead Delta emptied into Christmas Bay when it and WGB were one contiguous bay system (Bartek et al, 1990; Taha and Anderson 2008). Sediment derived from the Brazos River are reddish brown to orange in color and generally are an oxidized, clay-rich mud, in contrast to the grey to black, anoxic WGB estuarine mud. Brazos River mud deposits have been identified within strata on the west end of WGB, Christmas Bay, the shoreface Holocene deposits offshore of Follets Island (Dellapenna et al, 2016; Lavery, 2014), and offshore of the western end of Galveston Island (Dellapenna person. com.). In this study, the Paleo-Brazos River (PBR) deposits were found within both the Terramar Beach canal and the Indian Beach Bayou storm-surge channel. The radiocarbon dates at the top of the Indian Beach Bayou PBR layer was dated at 5033-5189 yBP and correlated to the SLP 27 core collected from (Lavery, 2014) at similar elevations. A sample collected from the top of the PBR layer of that core was dated at 4365-4416 yBP. Both cores contain PBR

deposits with similar thicknesses, but the top of the sediment layer has a 1,000-year difference, suggesting erosion occurred at the surface of the Indian Bayou PBR deposit.

The PBR surface was interpreted within the incised-valleys but was not present in sediment cores or seismic data collected in topographically high areas between valleys, suggesting that the antecedent topography had an influence on the distribution of the PBR deposits. The PBR deposits identified in this study were only found in the western side of WGB and Carancahua Reef. The average thickness of the PBR deposits is 2 m with a roughly uniform distribution within the incised-valley and topographically low areas. The areas with a high paleo-topographic relief have no PBR deposits, likely due to erosion or non-deposition. In **Figure 21**, the blacked-out areas on the map are areas that were topographic highs at the time of the PBR deposition and were not able to preserve the fluvial deposits. Given that the areas with high paleo-topographic relief have no PBR deposits, it indicates that the paleo-WGB was shallow and the lack of identified PBR deposits east of Carancahua Reef suggests that either a paleo-reef or the antecedent feature the reef sits provided a barrier for dispersal of the PBR sediment east of Carancahua Reef (**Fig. 22**). **Figure 22** shows a modified PBR path compared to a previously interpreted path by Anderson (2007) showing an extension of the Big Slough paleo river mouth.

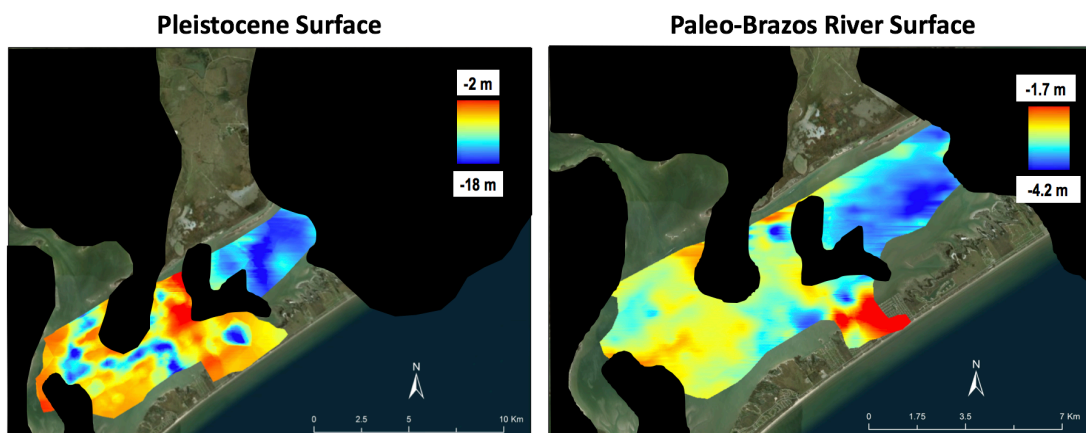


Figure 21. The Pleistocene Unconformity surface and the Paleo-Brazos River sediment distribution. The black outline marks the high topographic areas.

This path was interpreted based on the distribution of the PBR deposits seen in the seismic data and cores within WGB and the fact that Galveston Island didn't form to Modern-day Carancahua Reef until around 2,600 yBP. The Paleo-Brazos River was only active this far north from 6,000-4,000 years ago, the river mouth couldn't have been isolated to a tidal inlet. This interpretation is loosely based, but it provides evidence that the previously interpreted Big Slough river mouth, active from 6,000-4,000 years ago, needs to be expanded to include the western half of WGB. After the PBR changed course to the south, WGB ceased to directly receive PBR sediment and the estuary began to accumulate black estuarine mud above the PBR deposits. With the fluvial sediment source gone, WGB became a large estuary, but was not full inundated until a major flooding event around 4,400 yBP (Lavery, 2014).

6.3 Geomorphology

6.3.1 Transgressive vs. Regressive Features

To address the question; did the placement of these incised-valleys have any influence on the geomorphology or formation of Galveston Island? The geomorphic features were observed and correlated to the underlying geology. Galveston Island is a barrier island with a variety of geomorphic features on the bay-side and interior topography that provides clues to the influences of the island's formation (Anderson, 2007). Beach ridges and swales are the primary regressive geomorphic features representing the progradation of the island. The eastern 32 km of Galveston Island contain prominent beach ridges along with storm surge channels which cut across the beach ridges (**Fig. 23**). The oldest and most prominent beach ridges and swales formed from 5,300-3,300 yBP as the island grew seaward, with the last of the ridges located 2 km west of Jamaica Beach (Morton, 1974). The ridges are in a linear, east-west configuration, with the ages

of formation decreasing in a seaward direction. The western 15 km of Galveston Island has the characteristics of a younger, transgressive barrier island and contains many breach sites and large storm surge channels (**Fig. 23**). Primitive age dating methods using microfossils taken from beach ridges on the bay shoreline suggests the transgressive side of the island began forming around 3,000 yBP, when the islands accretionary stage began to decrease, and stopped around 1,800-1,200 yBP (Morton, 1974). The transition from regressive to transgressive features occurs on the western side of Jamaica Beach. Transgressive features extend to the western-most 17 km of the island, with a narrower width and no beach ridges.



Figure 22. Interpreted Path of PBR. The path of the Paleo-Brazos River (yellow) compared to previously interpreted river paths (Modified from Anderson, 2007)

The 1954 aerial photographic mosaics from Google Earth show the island with little to no infrastructure or development and unaltered geomorphic features. (**Fig. 23a**) The 1954 photos

reveal large storm surge channels further east on Galveston Island (e.g. Echert, Ganges, Syndor Bayous as well as Sweetwater Lake) that cut through older beach ridges, created during an earlier stage of island formation, dating around 5,300 yBP (Rodriguez et al, 2004). A younger set of beach ridges, seaward of the older set, are not cut by storm surge channels, suggesting they formed after the island was too wide to be breached by storm surge channels. These younger, prominent abandoned beach ridges were formed before the sea level reached a standstill around 3,000 yBP, signifying a period of barrier island growth (Morton, 1974). The sea level standstill occurred when the island transitioned from a regressive to transgressive mode of development. The storm surge channels located on the western-most 10 km of Galveston Island are younger channels formed by severe storm surge and overwash. This section of the island is narrower and lower in elevation, allowing storm surge to easily breach the island.

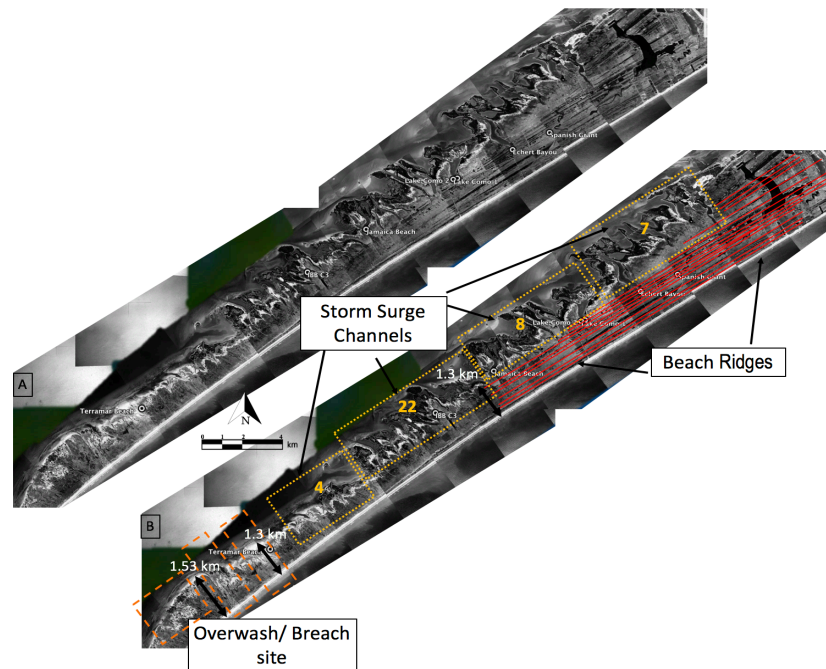


Figure 23. Geomorphic Features of Galveston Island. A. An uninterpreted aerial mosaic of Galveston Island. B. 1954 mosaic image with interpreted geomorphic features of Galveston Island. Red lines are beach ridges. Dotted yellow outlines areas are storm surge channels with the number of channels within the highlighted area. Orange dashed areas are overwash sites. Black arrows and white text represents the island widths.

6.3.2 Enhanced Subsidence Over Incised-Valleys and Bay Shoreline Retreat

The Trinity River Incised-Valley extends under the Trinity Bay portion of upper Galveston Bay (Rodriguez et al, 2005) and is filled with up to 30 m of Holocene estuarine and fluvial deposits. Pekowski (2017) observed sedimentation rates are up to 3 times as high within the incised-valley compare to areas within the bay, directly adjacent, but outside of the area underlined by the incised-valley. He concluded that this was an indication of highly localized subsidence in areas above the incised-valley, due to differential compaction of the Holocene fill. In the study of the Trinity River Incised-Valley, no cores were collected to measure the geotechnical properties of the Beaumont Formation because its surface was too deep to reach with vibracores, however, inferences were made in regard to the relative shear strength and compressive strength of the Beaumont Formation, in comparison to the unconsolidated Holocene fill. In WGB, the shear strength of the Beaumont Formation ranges between 0.7-1.0 kg cm⁻², in contrast to 0.10 to 0.02 kg cm⁻² for the Holocene fill, making the shear strength of the Beaumont Formation between 5 and 17.5 times higher than the Holocene fill. This means that the Beaumont Formation is indurated, highly compacted, and extremely resistant to erosion compared to the Holocene fill, which is relatively uncompacted and highly susceptible to erosion. The compressive strength showed similar results with the Pleistocene sediment being a magnitude higher at 0.13-0.22 kg cm⁻² compared to the Holocene sediment with 0.06-0.08 kg cm⁻². The Pleistocene sediment was harder to compress than the Holocene sediment, making it easily susceptible to subsidence.

Along the EWGB back-bay shoreline, the Pleistocene unconformity is about -5 to -10 m below the bay bottom. The extremely higher shear strength of the Beaumont Formation accounts for lack of significant compaction and the lack of localized subsidence occurring outside of the

areas above the incised-valley, where the Beaumont Formation surface is shallow. In contrast, the areas overlying the incised-valleys sit atop up to 12 m of unconsolidated, low shear strength sediment. This permits continual compaction, allowing for a higher degree of highly localized subsidence directly over the channels and differential compaction between the areas over the incised-valley versus areas where there are no subsurface incised-valleys. Areas along the bay shoreline with higher rates of subsidence should also have higher rates of bay shoreline retreat.

In the analyses of the shoreline retreat above the incised paleo-valleys, the shoreline retreat was significantly higher compared to areas with no incised-valley in the subsurface. The elevated shoreline retreat rates in areas above incised-valleys in the subsurface supports the assertion that sediment under the embayment has undergone greater subsidence. This is a result of differential compaction of the Holocene fill and the higher degree of subsidence over the incised-valleys is likely the cause of the retreat of the shoreline and the formation of embayments.

6.3.3 Storm Surge Channels

The three phases of island formation, from east to west, were mapped based on the geomorphic features and beach ridge radiocarbon dates from previous studies and interpretations (Bernard et al, 1959, Bernard et al, 1970, Morton, 1974). Once the subsurface geology was mapped, it was overlaid with the geomorphic phases of island development. The channel interpretations show a correlation between the locations of these channels and the geomorphic phases of the island formation (**Fig. 23b & Fig. 25**). The channels extend seaward in three areas throughout Galveston Island exactly where the island exhibits changes in topographical features and formation. The changes at these areas are evidence of how the channels have influenced the

phases of the islands accretion. The oldest section extends from the eastern end of the island to the western side of the HBIV, where the set of beach ridges is lower and the number of storm surge is higher. The island width decreases from 1.7 km to 1.4 km west of the HBIV. The 2nd phase of formation begins on the western side of HBIV and extends to the western side of the EHBIV. The western side of the HBIV marks the location where the island switches from regressive to transgressive geomorphology and decreases in width to 1.35 km (**Fig. 23b**). The disappearance of beach ridges and decrease in width is the main observation of this change in features. West of the EHBIV, at Maggies Cove, the island began its final phase of growth, with the island width decreasing and the only section containing modern and episodically active overwash. At the overwash site, the island has a width of 1.3 km. There is an increase in island width up to 1.53 km at the west end of Galveston Island (**Fig. 23b**). This area frequently changes due to its proximity to the tidal inlet, San Luis Pass. The HBIV once flowed through present-day Jamaica Beach and Carancahua Cove before this section of the barrier island was established ~2,600 yBP. **Figure 24** shows an interpreted path made from the observations of the topography and island formation. The 1954 aerial photo mosaic (**Fig. 24a**) reveals a large embayment forming Carancahua Cove and contains six storm surge channels where the canals of Jamaica Beach now exist. In the case of the HBIV channel, it was incised down to -10 m. Because the Holocene deposits are far more susceptible to both erosion and compaction than the surrounding Pleistocene terraces. Carancahua Cove and the other coves and embayments along the northern shore of Galveston Island, which sit above incised-valleys, are likely formed as a result of differential compaction of the overlying Holocene fill sediment, which would both enhance subsidence and shoreline erosion since the sediment is more susceptible to erosion. In addition to differential compaction within the incised-valleys, elevated subsidence, their association with

shoreline embayments, and the lower shear strength ($<0.1 \text{ kg cm}^{-2}$) of the Holocene sediment fill makes them zones of relative weakness. This weakness makes the filled incised-valleys are far more susceptible to erosion, creating fairways along the island's bay shoreline that are more vulnerable to the formation of storm surge channels. CIV/EHBIV is located below present-Maggies Cove and Bird Island Cove (**Fig. 24b**). The bay-side of the island in this area contains six storm surge channels and two large embayments. This last section of the island was established after 3,000 yBP until 1,800-1,200 yBP. These embayments formed atop incised-valleys, with the same processes described above having led to their formation.

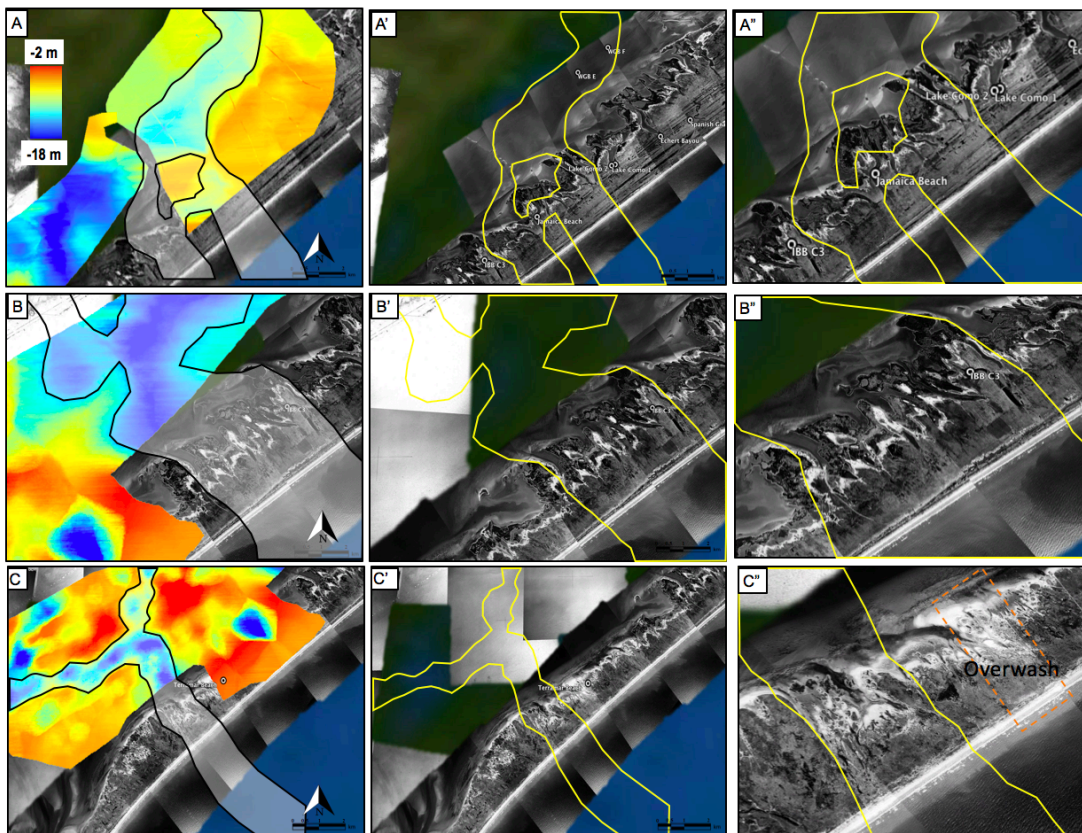


Figure 24. Interpreted Path of the Incised-Valleys beneath Galveston Island. A & A''. Interpreted path of the Highland Bayou Incised-Valley beneath Galveston Island. Interpreted path of the Highland Bayou Incised-Valley beneath Galveston Island over a 1954 aerial image. B-B''. Interpreted path of the Carancahua and Eastern Halls Bayou Incised-Valley beneath Galveston Island over a 1954 aerial image. C-C''. Interpreted path of the Highland Bayou Incised-Valley beneath Galveston Island. Interpreted path of the Chocolate Bayou Incised-Valley beneath Galveston Island over a 1954 aerial image.

CBIV lies below the west end of Galveston Island, which is the youngest section of the island, forming around 1,800 yBP (**Fig. 24c**). This section of the island contains two large storm surge channels with two washover fans.

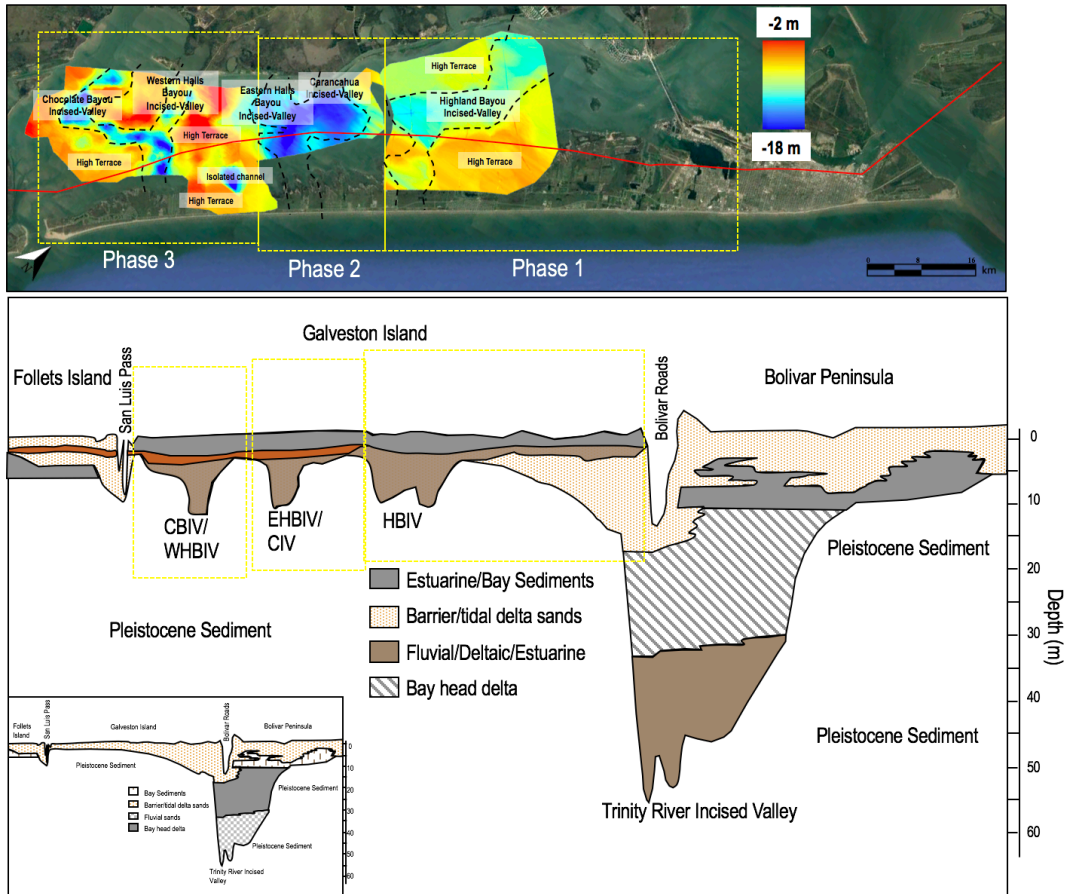


Figure 25. Cross-Section from Follets Island to Bolivar Peninsula. A cross-section of Bolivar Peninsula to Follets Island showing the thickness of the Holocene and how it is distributed atop the Beaumont Formation with the incised-valleys of WGB, and the Holocene stratigraphic record (Modified from Wallace et al, 2010).

Based on visual observations from 1954 aerial photo mosaics, there are 41 identified storm surge channels on the bay-side of Galveston Island, ranging from 50-250 m wide, generally extending 1-1.25 km into the interior of the island from the bay shoreline. There may be more, but were not easily identified. These storm surge channels cut through the island,

generally perpendicular to the shoreline, and carve through beach ridges during strong storm surge overwash. Along the eastern 32 km of Galveston Island, all of the storm surge channels terminate along the same beach ridge (**Fig. 23**), which dates to 3,300 yBP (Morton, 1974). These storm surge channels range from 900-1200 m long, suggesting that once the island exceeded this width (~1200 m), it was too wide to be breached by storm surge. Echert Bayou is one of 41 identified storm surge channels on the bay-side of Galveston Island and does not have an incised-valley beneath it, forming directly above consolidated barrier sediment (**Fig. 17a**). The base of the Echert Bayou storm surge channel is at -3.5 m below MSL. If the depth of the storm surge channel was -1.5 to -2 m below MSL, which would be roughly consistent with what has been found on Follets Island, then the Echert Bayou storm surge channel would have been formed when MSL was -2 to -2.5 m below where it is today, making its formation occurring around 3,000-4,500 yBP, when correlated to the Milliken sea level curve (**Fig. 26**).

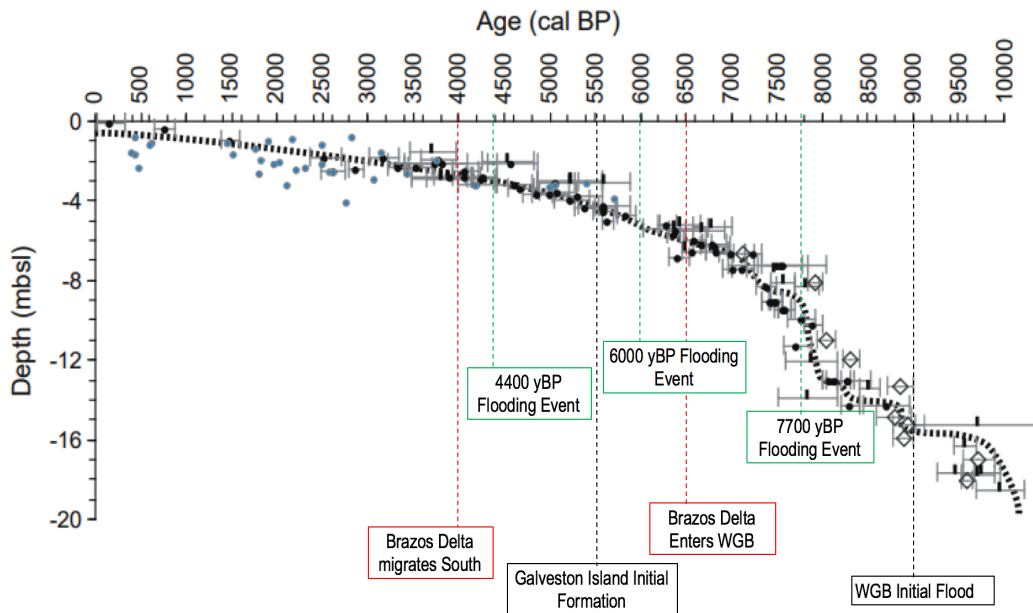


Figure. 26. Sea Level Curve. This sea level curve showing rising sea level during the Holocene transgression (Modified from Milliken et al, 2008).

This timing of formation is consistent with the channels forming approximately at the time of original formation of the regressive phase of the barrier island (3,000 yBP). The storm surge channel located at Jamaica Beach (**Fig. 17b**) has a depth of -2 m below MSL. According to Morton (1974), this section of the island was established between 2,600-3,000 yBP, when MSL was ~2 m below modern levels. This suggests that the base of the Jamaica Beach storm surge channel was approximately at MSL at the time of formation, which is consistent with the smaller storm surge channels observed on Follets Island.

7. CONCLUSIONS

The Pleistocene surface beneath WGB consists of the Beaumont and Deweyville Terraces (−9 m and −9.5 m) and a network of both simple, coastal plain and compound piedmont incised-valleys. The compound, piedmont incised-valleys (CBIV and EHBIV) were likely formed by the Brazos River during Stage 5e (~120 kya) when the paleo-river formed a delta within the area currently occupied by WGB (Anderson et al, 2016). The presence of the Deweyville terraces provide evidence that the compound incised-valleys beneath WGB formed at the same time and were influenced by the same sea level fluctuations as the Trinity River Incised-Valley. The Deweyville Terraces influenced the accommodation space within the incised-valleys by widening them through aggradation. The simple incised-valleys (WHBIV, CIV, and HBIV) are coastal-plain incised-valleys, likely formed during the late Pleistocene and are associated with smaller drainage basins, as evidenced by the narrower cross-sections, widths, and their shallower incision depths.

During the Early Holocene, as sea level rose, these Pleistocene incised-valleys became the earliest estuaries within the paleo-WGB system with, according to Lavery (2014), the first estuarine sediments began appearing around 9,000 yBP. As sea level continued to rise these valleys continued to fill with estuarine muds. The PBR flowed through a section of the western half of WGB from 4,000-6,000 yBP, depositing a clearly identifiable bayhead delta across the western half of WGB. Carancahua Reef provided a barrier that prevented it from flowing into the eastern half of WGB. The absence of PBR deposits on some of the topographically high areas within the bay suggests that these areas were subaerially exposed during shallow water levels and provided the preservation of mud deposits. The presence of the PBR under the western half of Galveston Island provides an additional time constraint for when that section of the island

formed. After the PBR channel changed course, the PBR sediment ceased to be deposited in WGB and a modern sequence of the WGB Estuarine facies was deposited, which continues today.

This study found that there are three major valleys that extend beneath Galveston Island, from east to west, they are: 1) The HBIV, 2) the CIV and EHBIV, and 3) the merged WHBIV and CBIV. The accommodation space the channels created acted as an obstacle the island had to overcome before it could continue to form. HBIV, CIV/EHBIV, and CBIV/WHBIV are placed beneath a section of the island that exhibits unique geomorphic features (storm surge channels, embayment size, presence of beach ridges and overwash). The islands width also decreases from east to west with each phase, noticeably at the site of where the channels are beneath the island.

The Beaumont Formation has a shear strength ranging between $0.7\text{-}1.0\text{ kg cm}^{-2}$, in contrast to $0.10\text{-}0.02\text{ kg cm}^{-2}$ for the Holocene fill, making the shear strength of the Beaumont Formation between 5 and 17.5 times as high as that of the Holocene fill. The compressive strength of the Beaumont sediment was $0.13\text{-}0.22\text{ kg cm}^{-2}$ and the Holocene sediment was less at $0.06\text{-}0.08\text{ kg cm}^{-2}$. The Pleistocene sediment was a magnitude higher with values of $0.7\text{ to }1\text{ kg cm}^{-2}$. Therefore, the Beaumont Formation is indurated, highly compacted, and is extremely resistant to erosion, whereas, the Holocene fill is relatively uncompacted and highly susceptible to erosion. As a result, the Holocene filled channels and valleys undergo differential compaction, resulting in enhanced subsidence and are easily eroded, compared to the Beaumont Formation. Consequently, the Holocene sediment filled valleys constitute geotechnically weak zones along the island. Their geotechnical weakness made these zones far more susceptible to the formation of storm surge channels. There are small storm surge channels along sections of the island where there are no mapped incised-valleys. However, along the western-most 20 km of the island, all of

the larger and deeper storm surge channels reside within the banks of Pleistocene incised-valleys, indicating that the presences of these valleys along Galveston Island appears to be a significant control on their distribution.

The initial formation of storm surge channels along the back-bay of Galveston Island began concomitant with the initial formation of Galveston Island, when it was in a narrower regressive phase and overwash and breaching were common occurrences. The island width reached a critical threshold where breaching was no longer possible, increasing to wider than 1,200 m around 3,300 yBP. This is discerned by beach ridges of this age that have never been breached by overwash channels.

This study addressed the hypothesis: Topographic variations of the antecedent Pleistocene surface of the WGB system was a major control during the formation and evolution of Galveston Island. The data collected for this study were used to understand the relationship between the antecedent topography and how its presence can influence the formation of a coastal environment specifically a barrier island. The dynamics involved in creating a coastal environment involve many different factors. To expand on this influence, more data needs to be collected to extend the valley findings to the shoreface and to stratigraphically interpret the new valleys for future research. This study raised more questions than it answered. Recommendations for future research would be to map out the paleo-valleys in more detail, to fill the gaps. More detail on the incised-valley path below Galveston Island to better understand their relationship locally and understanding how antecedent topography can influence other barrier islands and coastal environments. In addition, better documentation on the geotechnical parameters of the stratigraphic units investigated as well as a mapping of the potential spatial heterogeneity of these properties. In addition, using available LiDAR data from the bay shoreline to determine if

there are actual differences in land elevation over the incised-valleys, coupled with marsh and bay cores both within and outside of the areas above the channels. This can be used to determine whether there are spatial variabilities within sedimentation rates that can be associated with the presumed enhanced subsidence above the buried valleys, following the same approach used by Pekowski (2017).

REFERENCES

- Ameratunga, J., Sivakugan, N., & Das, B. M. (2016). Vane Shear Test. In *Correlations of Soil and Rock Properties in Geotechnical Engineering* (pp. 193-205). Springer, New Delhi.
- Anderson, J. B. (2007). *The Formation and Future of the Upper Texas Coast: A Geologist Answers Questions about Sand, Storms, and Living by the Sea* (Vol. 11). Texas A&M University Press.
- Anderson, J. B., Rodriguez, A., Abdulah, K. C., Fillon, R. H., Banfield, L. A., Mckeown, H. A., & Wellner, J. S. (2004). Late Quaternary stratigraphic evolution of the northern Gulf of Mexico margin: a synthesis.
- Anderson, J. B., Davidson, M., Geissman, J. W., Hampson, G. J., Reed, D. J., & Törnqvist, T. E. (2013). Coastal processes and environments under sea-level rise and changing climate: science to inform management. *GSA Today*, 23, 16-17.
- Anderson, J. B., Wallace, D. J., Simms, A. R., Rodriguez, A. B., & Milliken, K. T. (2014). Variable response of coastal environments of the northwestern Gulf of Mexico to sea-level rise and climate change: Implications for future change. *Marine Geology*, 352, 348-366.
- Anderson, J. B., Wallace, D. J., Simms, A. R., Rodriguez, A. B., Weight, R. W., & Taha, Z. P. (2016). Recycling sediments between source and sink during a eustatic cycle: Systems of late Quaternary Northwestern Gulf of Mexico Basin. *Earth-Science Reviews*, 153, 111-138.
- Bartek, L. R., Anderson, J. B., & Abdulah, K. C. (1990). The importance of overstepped deltas and interfluvial sedimentation in the transgressive systems tract of high sediment yield

- depositional systems—Brazos–Colorado deltas, Texas. In *Sequence Stratigraphy as an Exploration Tool: Concepts and Practices in the Gulf Coast: SEPM, Gulf Coast Section, 11th Annual Research Conference, Program and Abstracts* (pp. 59-70).
- Belknap, D. F., & Kraft, J. C. (1985). Influence of antecedent geology on stratigraphic preservation potential and evolution of Delaware's barrier systems. *Marine geology*, 63(1-4), 235-262.
- Bernard, H. A. (1950). Quaternary Geology of Southeast Texas.
- Bernard, H. A., C. Major Jr, and B. Parrott. 1959. The Galveston barrier island and environs: a model for predicting reservoir occurrence and trend.
- Bernard, H. A., LeBlanc, R. J., & Major, C. F. (1962). Recent and Pleistocene Geology of Southeast Texas: Field Excursion No. 3, November 10 and 11.
- Bernard, H., C. Major Jr, B. Parrott, and R. Leblanc. 1970. Recent sediments of southeast Texas—a field guide to the Brazos alluvial and deltaic plains and the Galveston barrier island complex.
- Brantley, S. T., Bissett, S. N., Young, D. R., Wolner, C. W., & Moore, L. J. (2014). Barrier island morphology and sediment characteristics affect the recovery of dune building grasses following storm-induced overwash. *PloS one*, 9(8), e104747.
- Blum, M. D., & Törnqvist, T. E. (2000). Fluvial responses to climate and sea-level change: a review and look forward. *Sedimentology*, 47(s1), 2-48.
- Blum, M. D., Misner, T. J., Collins, E. S., Scott, D. B., Morton, R. A., & Aslan, A. (2001). Middle Holocene sea-level rise and highstand at+ 2 m, central Texas coast. *Journal of Sedimentary Research*, 71(4), 581-588.

- Blum, M. D., & Aslan, A. (2006). Signatures of climate vs. sea-level change within incised valley-fill successions: Quaternary examples from the Texas Gulf Coast. *Sedimentary Geology*, 190(1-4), 177-211.
- Blum, M. D., Morton, R. A., & Durbin, J. M. (1995). "Deweyville" Terraces and Deposits of the Texas Gulf Coast: A Reevaluation. *Transactions-Gulf Coast Association of Geological Societies*, 53-60.
- Blum, M. D., & Price, D. M. (1998). Quaternary alluvial plain construction in response to glacio-eustatic and climatic controls, Texas Gulf coastal plain.
- Bureau of Economic Geology. (n.d.). Retrieved from <http://www.beg.utexas.edu/thscmp-environment>
- Carter, R. W. G., & Woodroffe, C. D. (1994). Coastal evolution: an introduction. *Coastal Evolution: late Quaternary shoreline morphodynamics*, 1-31.
- Dalrymple, R. W., Zaitlin, B. A., & Boyd, R. (1992). Estuarine facies models: conceptual basis and stratigraphic implications: perspective. *Journal of Sedimentary Research*, 62(6).
- Dalrymple, R. W. (1994). *Incised-valley systems: origin and sedimentary sequences* (No. 51). Sepm Society for Sedimentary.
- Dalrymple, R. W., Boyd, R., & Zaitlin, B. A. (1994). History of research, types and internal organisation of incised-valley systems: introduction to the volume.
- Davis, R. A. (1994). Barrier island systems—a geologic overview. In *Geology of Holocene barrier island systems* (pp. 1-46). Springer, Berlin, Heidelberg.
- Davis Jr, R. A., & FitzGerald, D. M. (2009). *Beaches and coasts*. John Wiley & Sons.
- Davis, R. A. (2012). Tidal signatures and their preservation potential in stratigraphic sequences. In *Principles of tidal sedimentology* (pp. 35-55). Springer Netherlands.

- Dellapenna, T. M., Carlin, J. A., Williams, J., Breedlove, L., McGuffin, A., Pekowski, A., Hill, L., 2016. Report to the Texas Coastal Management Program: CMP Cycle 17 Follets Island Offshore Coring Supplement: Final Report: If We Lose Follets Island We Lose Coastal Communities and Christmas Bay: A Geological Framework Study and Numerical Model Study of the Sustainability of Follet's Island. 94 p.
- Flint, R. F. (1957). Glacial and Pleistocene geology: John Wiley & Sons. *Inc., New York*, 5.
- Garcia, T. D. (1991). Environmental Impact of Clays Along the Upper Texas Coast. *Environmental Impact of Clays Along the Upper Texas Coast*, 1.
- Gibeaut, J. C., Waldinger, R., Hepner, T., Tremblay, T. A., White, W. A., & Xu, L. (2003). Changes in bay shoreline position, west bay system, Texas. *Report of the Texas Coastal Coordination Council Pursuant to National Oceanic and Atmospheric Administration Award No. NA07OZ0134 GLO Contract No.*
- Gibling, M. R. (2006). Width and thickness of fluvial channel bodies and valley fills in the geological record: a literature compilation and classification. *Journal of sedimentary Research*, 76(5), 731-770.
- Hayes, M. O. (1966). Sedimentation on a semiarid, wave-dominated coast (South Texas) with emphasis on hurricane effects.
- Hays, J. D., Imbrie, J., & Shackleton, N. J. (1976, December). Variations in the Earth's orbit: pacemaker of the ice ages. Washington, DC: American Association for the Advancement of Science.
- Houser, C., Hapke, C., & Hamilton, S. (2008). Controls on coastal dune morphology, shoreline erosion and barrier island response to extreme storms. *Geomorphology*, 100(3), 223-240.

- Lavery, 2014. Topographic and Base-level Control of Back-Barrier Lagoon Evolution: West Galveston Bay, Texas. (Unpublished Thesis)
- McNinch, J. E. (2004). Geologic control in the nearshore: shore-oblique sandbars and shoreline erosional hotspots, Mid-Atlantic Bight, USA. *Marine Geology*, 211(1-2), 121-141.
- Milliken, K. T., Anderson, J. B., & Rodriguez, A. B. (2008). A new composite Holocene sea-level curve for the northern Gulf of Mexico. *Geological Society of America Special Paper*, 443, 1-11.
- Morton, R. A. (1994). Texas barriers. In *Geology of Holocene Barrier Island Systems* (pp. 75-114). Springer Berlin Heidelberg.
- Morton, R. A. (1974). *Shoreline changes on Galveston Island (Bolivar Roads to San Luis Pass): An analysis of historical changes of the Texas Gulf shoreline*. University of Texas, Bureau of Economic Geology.
- Morton, R. A. (2002). Factors controlling storm impacts on coastal barriers and beaches: a preliminary basis for near real-time forecasting. *Journal of Coastal Research*, 486-501.
- Morton, R. A., & McGowen, J. H. (1980). *Modern depositional environments of the Texas coast*. University of Texas at Austin, Bureau of Economic Geology.
- Nordfjord, S., Goff, J. A., Austin Jr, J. A., & Sommerfield, C. K. (2005). Seismic geomorphology of buried channel systems on the New Jersey outer shelf: assessing past environmental conditions. *Marine Geology*, 214(4), 339-364.
- Oertel, G. F. (1985). The barrier island system. *Marine Geology*, 63(1-4), 1-18.
- Pekowski, A. (2017). Elevated modern sedimentation rates over the buried Trinity River incised valley suggests elevated, localized subsidence rates, Galveston Bay, TX, USA. Unpublished MS Thesis, Texas A&M University.

- Posamentier, H. W., & Allen, G. P. (1993). Variability of the sequence stratigraphic model: effects of local basin factors. *Sedimentary geology*, 86(1-2), 91-109.
- Rodriguez, A. B., Fassell, M. L., & Anderson, J. B. (2001). Variations in shoreface progradation and ravinement along the Texas coast, Gulf of Mexico. *Sedimentology*, 48(4), 837-853.
- Rodriguez, A. B., Anderson, J. B., Siringan, F. P., & Taviani, M. (2004). Holocene evolution of the east Texas coast and inner continental shelf: along-strike variability in coastal retreat rates. *Journal of Sedimentary Research*, 74(3), 405-421.
- Rodriguez, A. B., Anderson, J. B., & Simms, A. R. (2005). Terrace inundation as an autocyclic mechanism for parasequence formation: Galveston Estuary, Texas, USA. *Journal of Sedimentary Research*, 75(4), 608-620.
- Schumm SA (1965) Quaternary paleohydrology. In: Wright HE Jr, and Frey DG (Eds), The Quaternary of the United States. Princeton: Princeton University Press, pp 783–794
- Schwab, W. C., Thieler, E. R., Allen, J. R., Foster, D. S., Swift, B. A., & Denny, J. F. (2000). Influence of inner-continental shelf geologic framework on the evolution and behavior of the barrier-island system between Fire Island Inlet and Shinnecock Inlet, Long Island, New York. *Journal of Coastal Research*, 408-422.
- Simms, A. R., Anderson, J. B., Taha, Z. P., & Rodriguez, A. B. (2006). Overfilled versus underfilled incised valleys: examples from the Quaternary Gulf of Mexico.
- Simms, A. R., Aryal, N., Miller, L., & Yokoyama, Y. (2010). The incised valley of Baffin Bay, Texas: a tale of two climates. *Sedimentology*, 57(2), 642-669.
- Stutz, M. L., & Pilkey, O. H. (2001). A review of global barrier island distribution. *Journal of Coastal Research*, 15-22.

- Taha, Z. P., & Anderson, J. B. (2008). The influence of valley aggradation and listric normal faulting on styles of river avulsion: a case study of the Brazos River, Texas, USA. *Geomorphology*, 95(3-4), 429-448.
- Wallace, D. J., Anderson, J. B., Rodriguez, A. B., Kelley, J. T., Pilkey, O. H., & Cooper, J. A. G. (2009). Natural versus anthropogenic mechanisms of erosion along the upper Texas coast. *America's Most Vulnerable Coastal Communities. The Geological Society of America Special Paper*, 460, 137-147.
- Wallace, D. J. (2010). *Response of the Texas coast to global change: Geologic versus historic timescales*. Unpublished Ph.D. Dissertation, Rice University
- Wallace, D. J., Anderson, J. B., & Fernández, R. A. (2010). Transgressive ravinement versus depth of closure: A geological perspective from the upper Texas coast. *Journal of Coastal Research*, 26(6), 1057-1067.
- Wallace, D. J., & Anderson, J. B. (2013). Unprecedented erosion of the upper Texas coast: Response to accelerated sea-level rise and hurricane impacts. *Geological Society of America Bulletin*, 125(5-6), 728-740.
- Zaitlin, B. A., Dalrymple, R. W., & Boyd, R. O. N. (1994). The stratigraphic organization of incised-valley systems associated with relative sea-level change.

APPENDIX

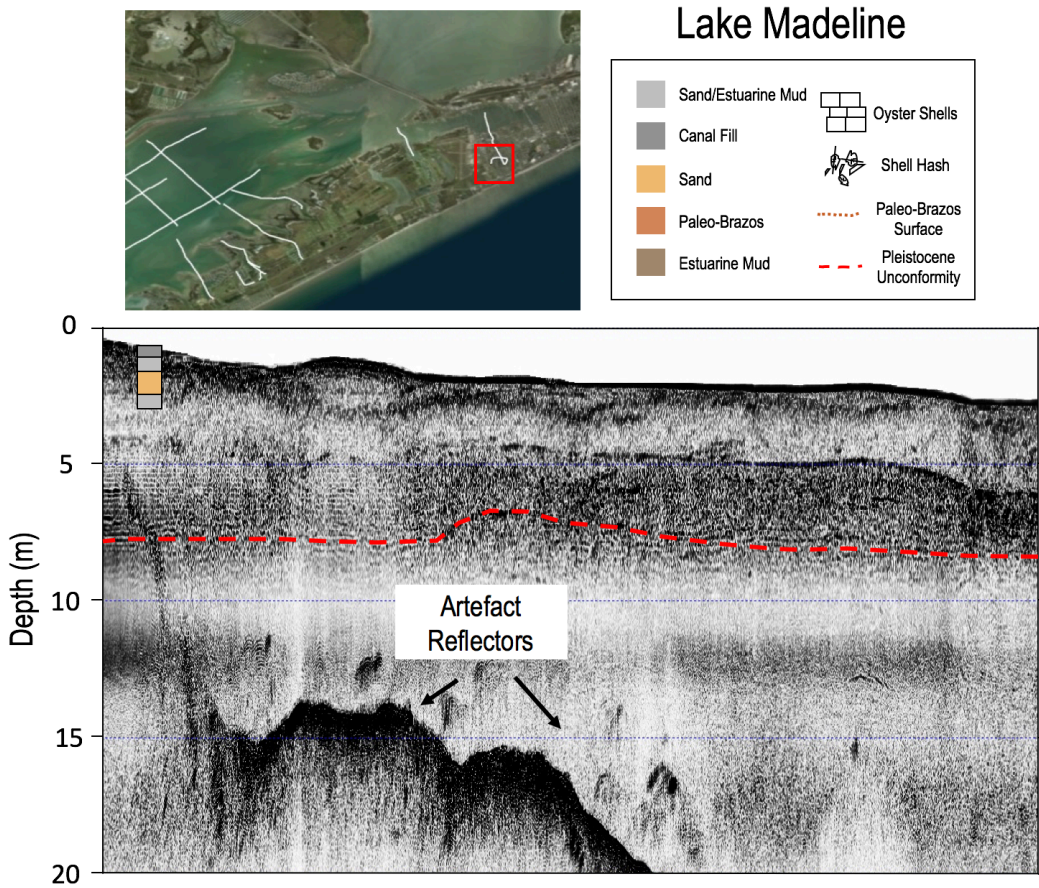


Figure A.1. Core lithology depicted over the seismic image in the Lake Madeline canal.



Spanish Grant

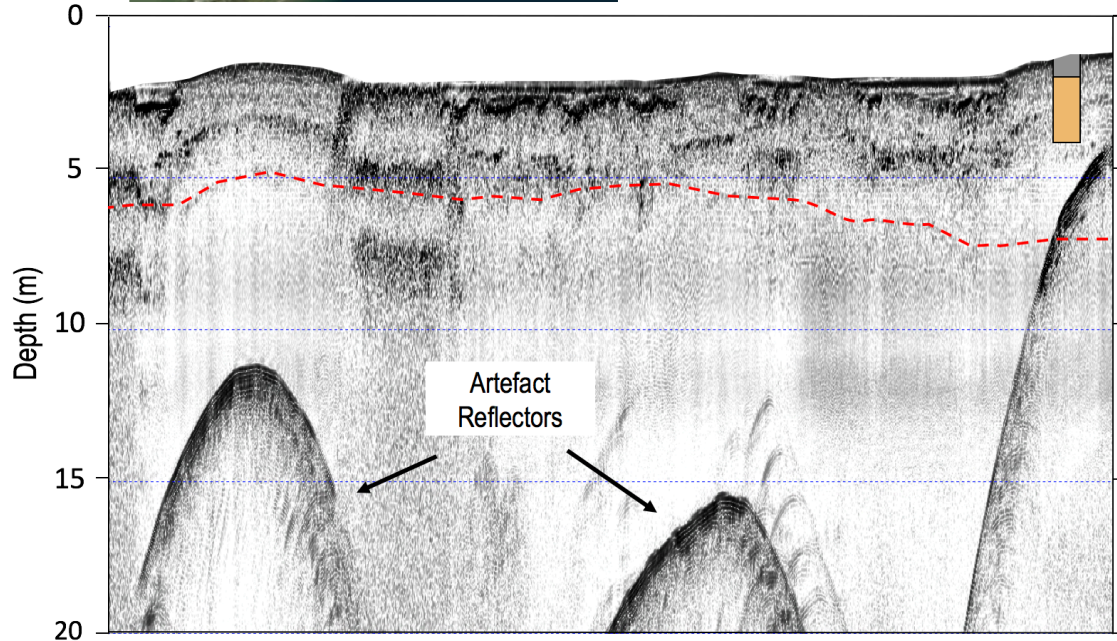
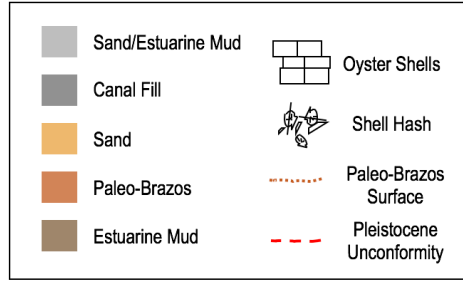


Figure A.2. Core lithology depicted over the seismic image in the Spanish Grant canal.

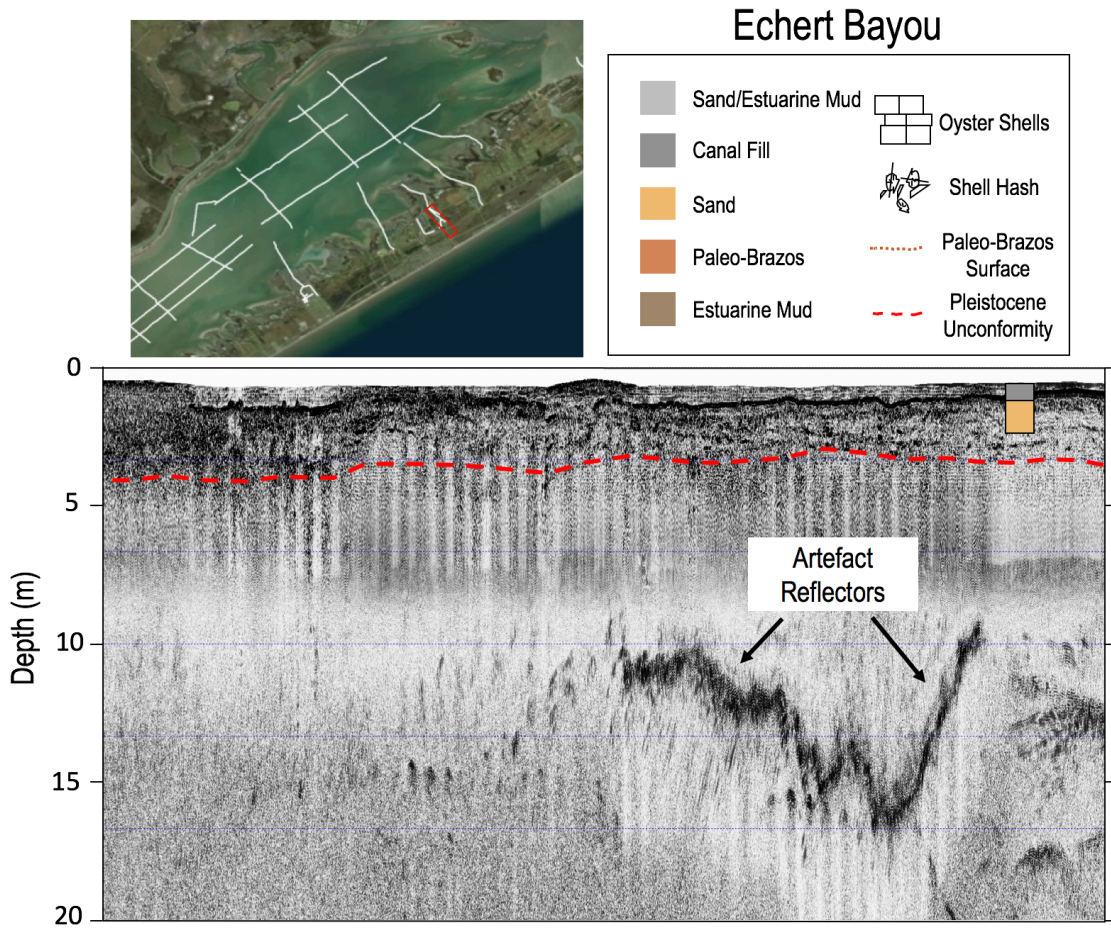


Figure A.3. Core lithology depicted over the seismic image in the Echert Bayou canal.

Lake Como 2

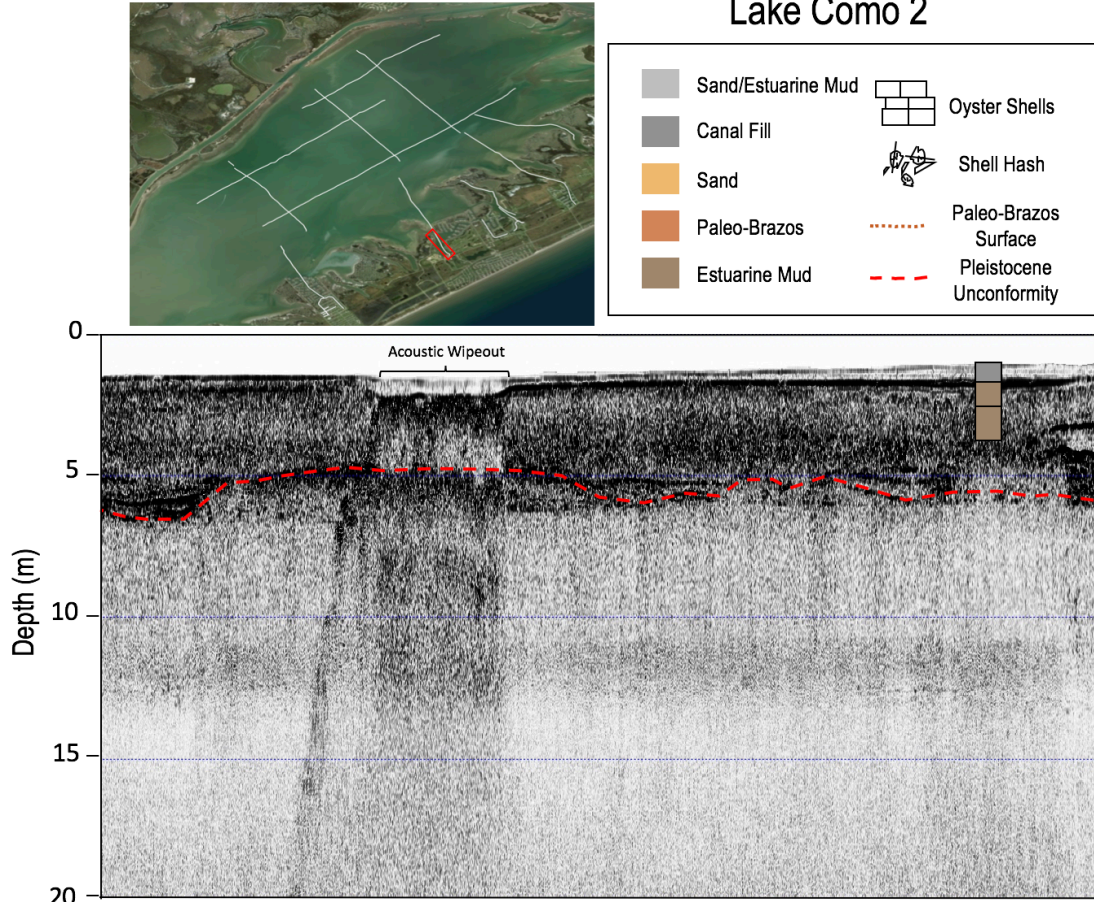


Figure A.4. Core lithology depicted over the seismic image in the Lake Como canal.

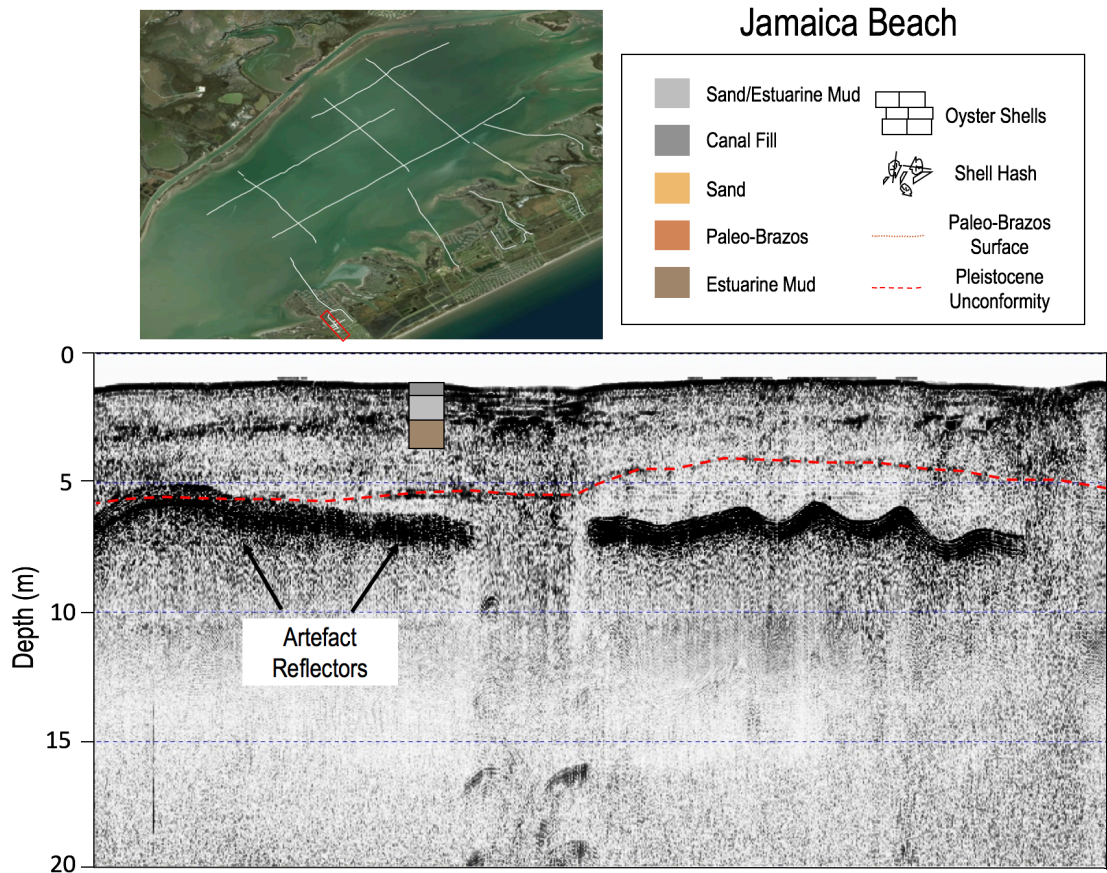


Figure A.5. Core lithology depicted over the seismic image in the Jamaica Beach canal.

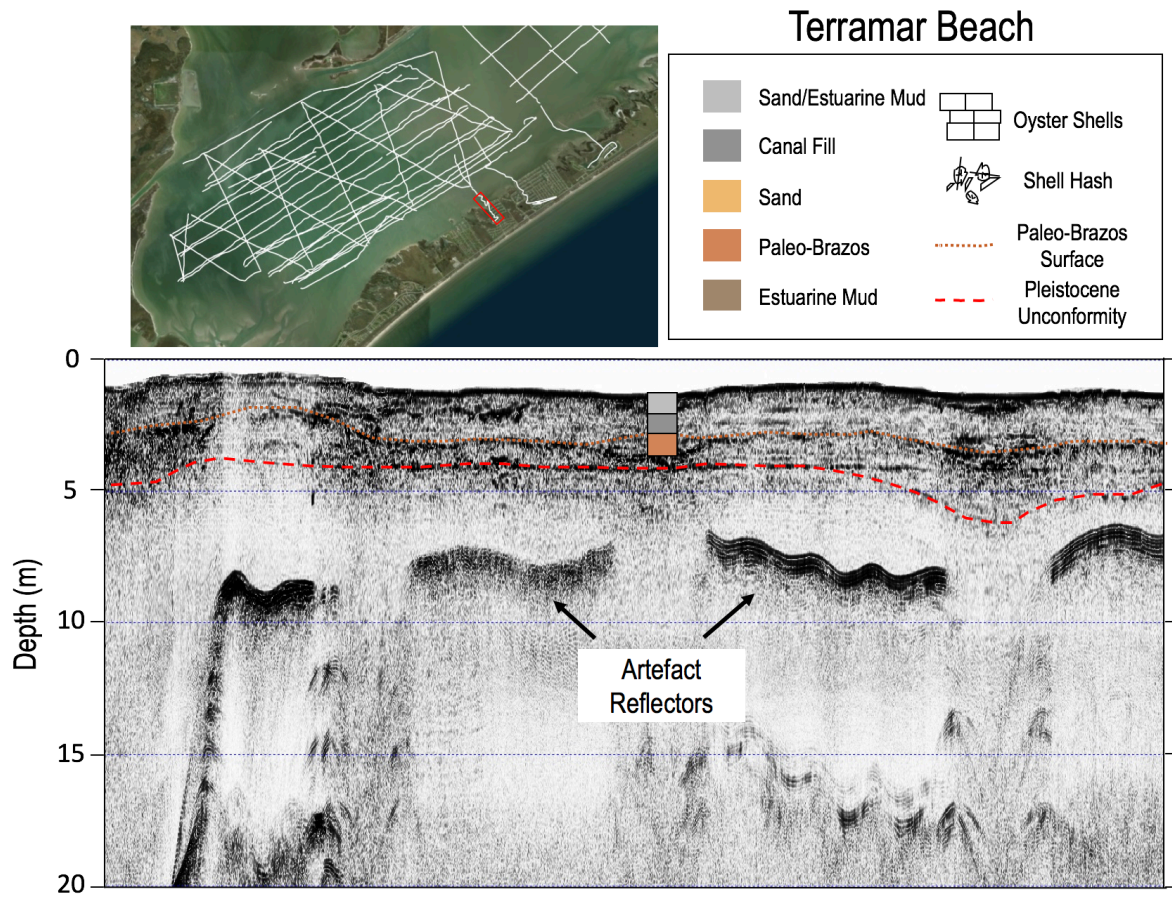


Figure A.6. Core lithology depicted over the seismic image in the Terramar Beach canal.

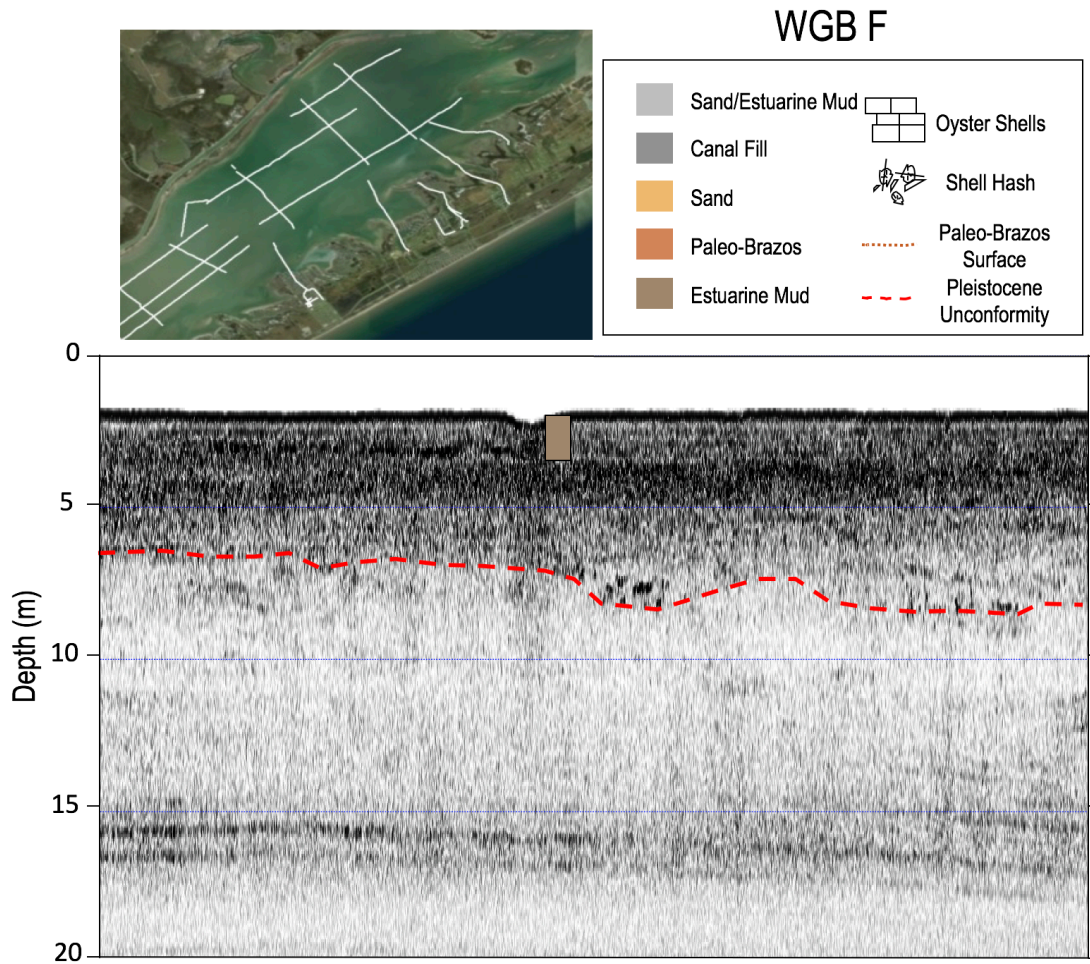


Figure A.7. Core lithology depicted over the seismic image of WGB F.

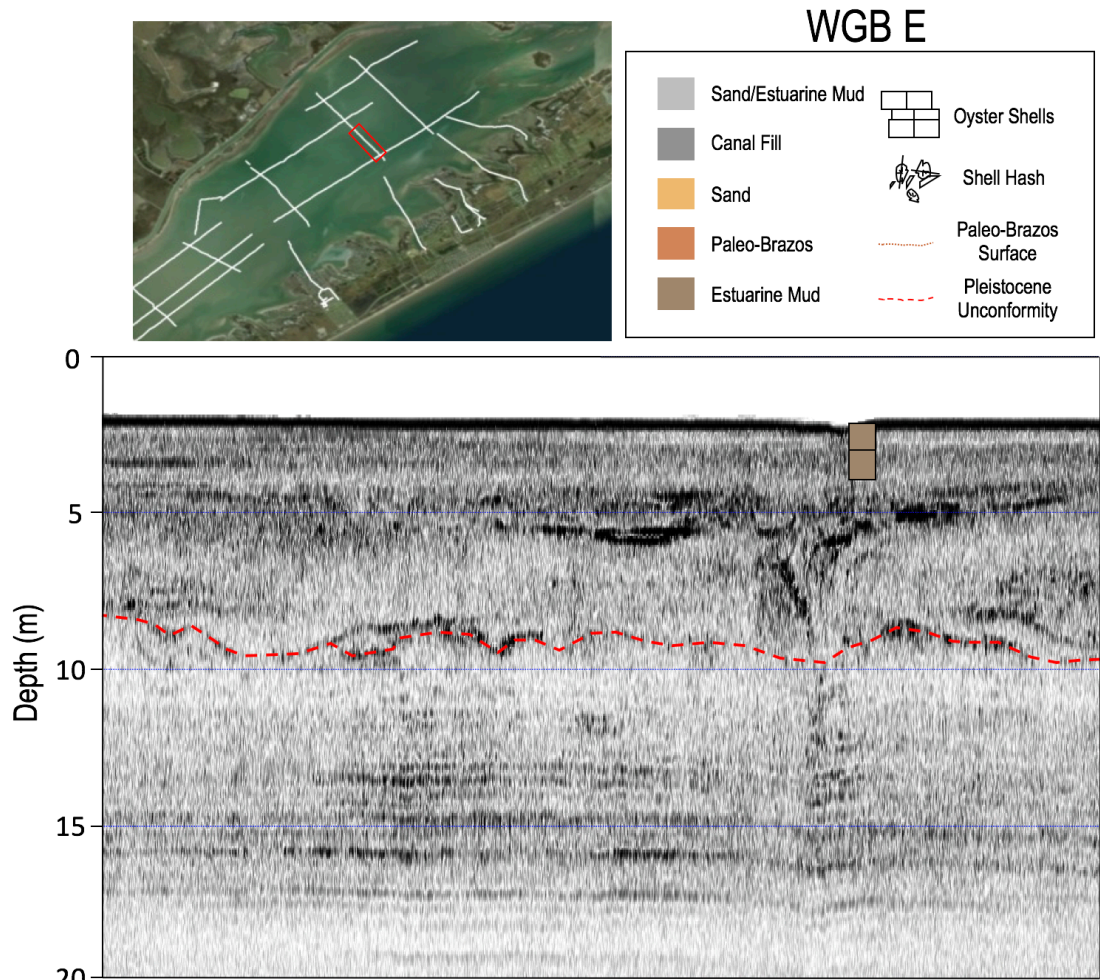


Figure A.8. Core lithology depicted over the seismic image of WGB E.

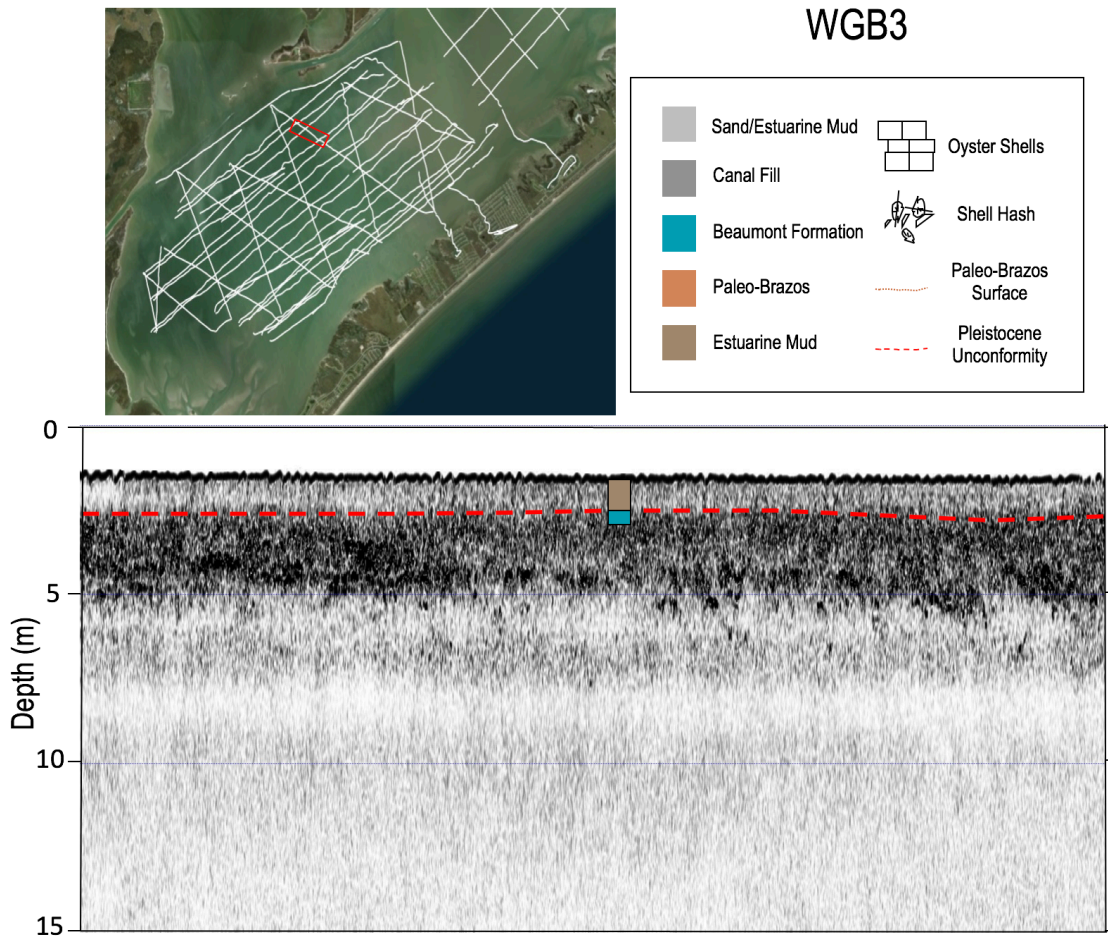


Figure A.9. Core lithology depicted over the seismic image of WGB3.

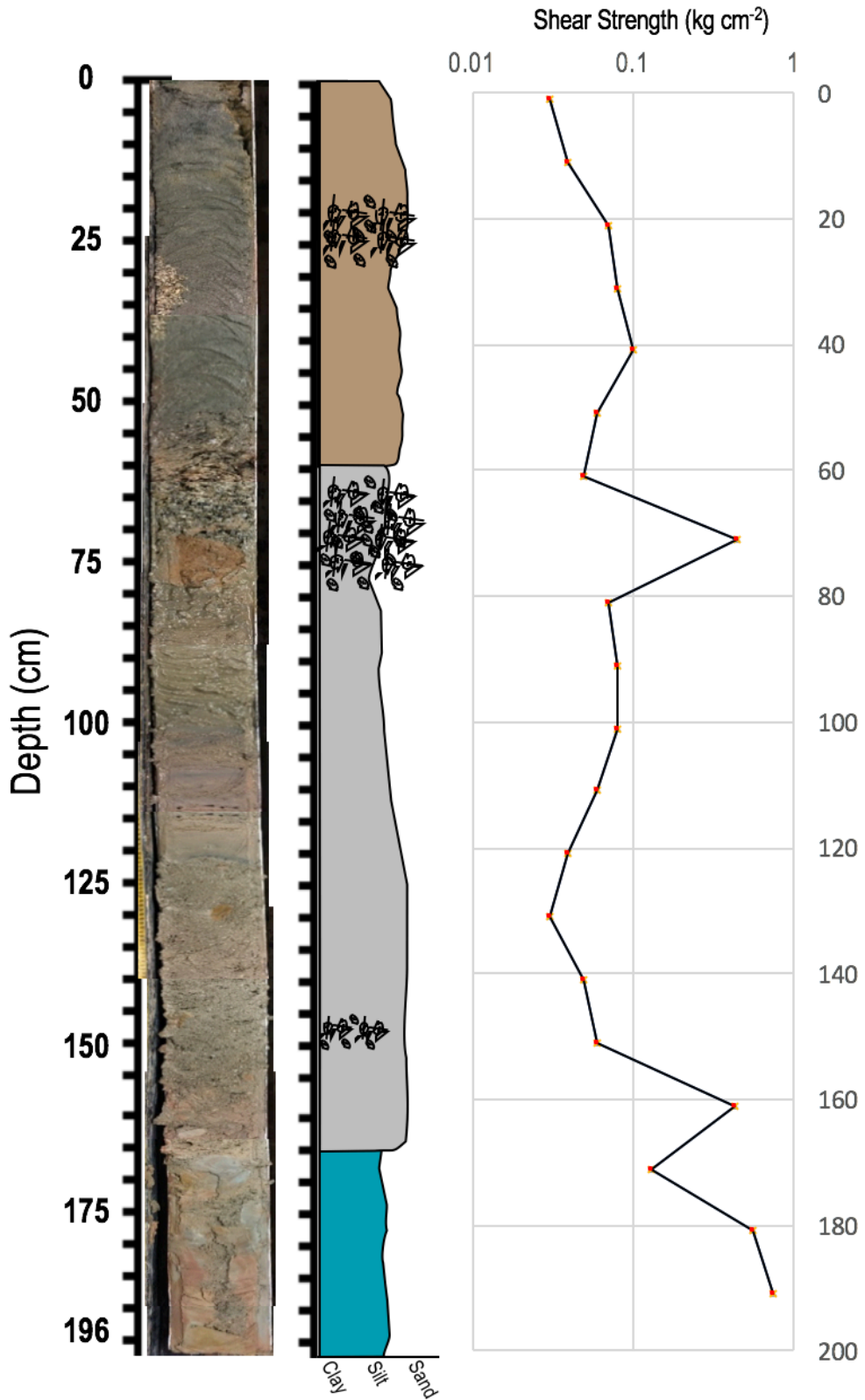


Figure A.10. Core Photo, Description and shear strength values of PIB-2

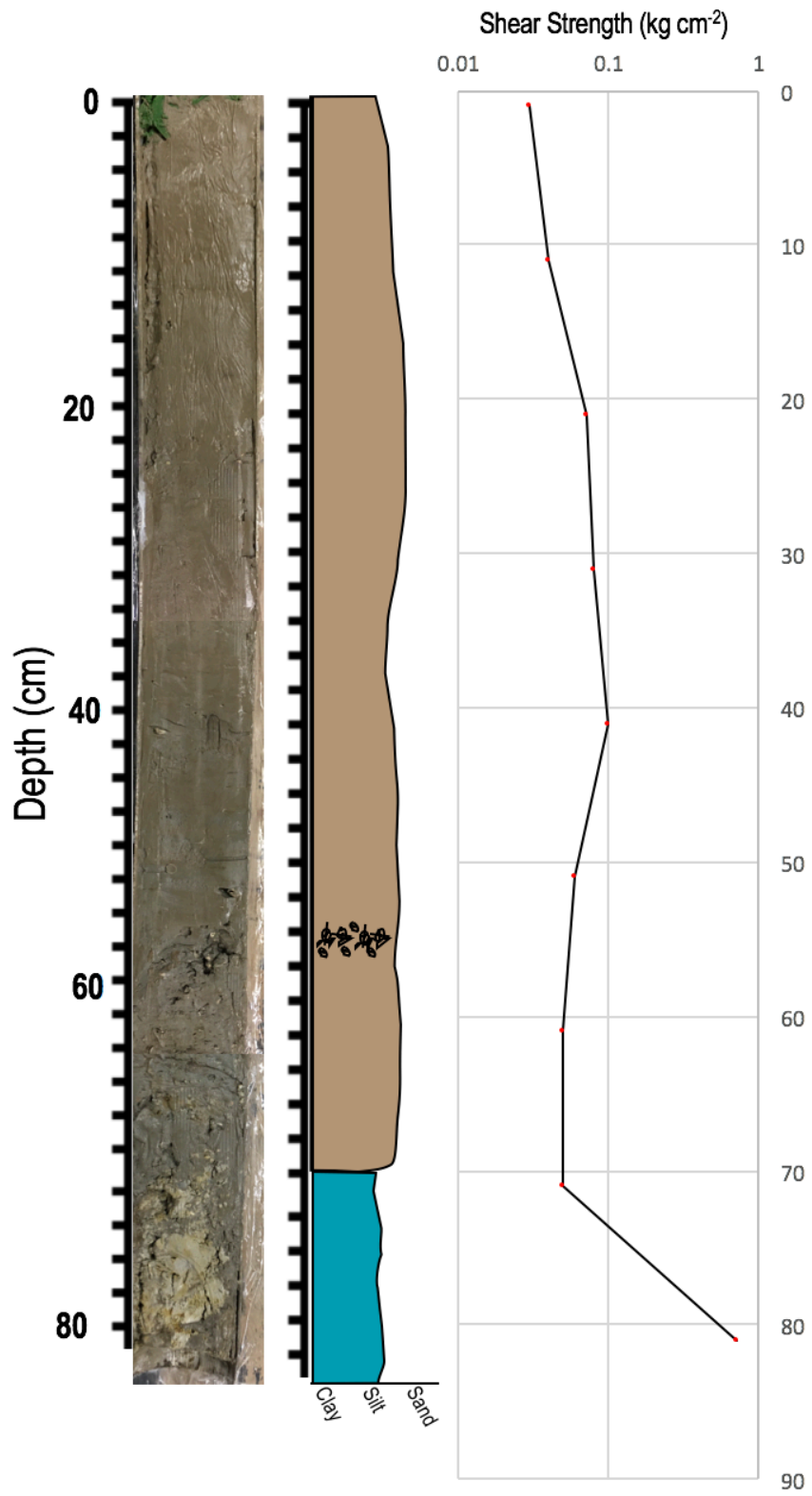


Figure A.11. Core Photo, Description, and shear strength values of WGB3

Table A.1. Core coordinates and lengths

Core Name	Latitude	Longitude	Length (m)
Lake Madeline	29°18'51.47"N	94°49'25.86"W	2.4
Spanish Grant	29°13'26.28"N	94°54'59.70"W	2.8
Echert Bayou	29°13'5.28"N	94°55'47.94"W	2.1
Lake Como 1	29°12'28.98"N	94°57'4.92"W	2.43
Lake Como 2	29°12'30.36"N	94°56'59.64"W	2.85
Jamaica Beach	29°11'28.44"N	94°58'56.58"W	1.96
Indian Beach	29°10'40.09"N	95° 0'10.19"W	5.4
Bayou C3			
Terramar Beach	29° 8'6.48"N	95° 3'46.80"W	2.65
WGB_E	29°14'31.56"N	94°57'55.44"W	1.56
WGB_F	29°15'6.96"N	94°57'5.58"W	0.84
WGB3	29° 9'34.56"N	95° 6'23.94"W	0.82
PIB-2	29°18'51.47"N	94°49'25.86"W	1.96

Table A.2. Shear Strength Results using the Pocket Torvane Shear Test Results of PIB-2

Depth (cm)	Test Value	Factor	Factored Value (kg cm⁻²)
1	0.13	0.2	0.03
11	0.20	0.2	0.04
21	0.35	0.2	0.07
31	0.40	0.2	0.08
41	0.51	0.2	0.10
51	0.30	0.2	0.06
61	0.24	0.2	0.05
71	0.44	1	0.44
81	0.33	0.2	0.07
91	0.41	0.2	0.08
101	0.41	0.2	0.08
111	0.30	0.2	0.06
121	0.20	0.2	0.04
131	0.14	0.2	0.03
141	0.23	0.2	0.05
151	0.30	0.2	0.06
161	0.43	1	0.43
171	0.13	1	0.13
181	0.23	2.5	0.56
191	0.30	2.5	0.75

Table A.3. Shear Strength Results using the Pocket Torvane Shear Test of WGB3

Depth (cm)	Test Value	Factor	Factored Value (kg cm⁻²)
1	0.15	0.2	0.03
11	0.14	0.2	0.04
21	0.13	0.2	0.07
31	0.19	0.2	0.08
41	0.14	0.2	0.10
51	0.10	0.2	0.06
61	0.10	0.2	0.05
71	0.10	0.2	0.05
81	0.70	1	0.70

Table A.4. Compressive Strength Results using the Pocket Penetrometer of WGB3

Depth (cm)	Test Value	Adapter	Factored Value (kg cm⁻²)
1	1.00	16	0.06
11	1.20	16	0.08
21	1.00	16	0.06
31	1.20	16	0.08
41	1.80	16	0.11
51	1.30	16	0.08
61	1.50	16	0.09
71	2.00	16	0.13
81	3.50	16	0.22